

10157
NACA TN 3804

NATIONAL ADVISORY COMMITTEE FOR AERONAUTICS



0066716

TECH LIBRARY KEEPS, NM

TECHNICAL NOTE 3804

A FACTOR AFFECTING TRANSONIC LEADING-EDGE FLOW SEPARATION

By George P. Wood and Paul B. Gooderum

Langley Aeronautical Laboratory
Langley Field, Va.



Washington

October 1956

AFMDC
TECHNICAL LIBRAR
AFL 2811



0066716

NATIONAL ADVISORY COMMITTEE FOR AERONAUTICS

TECHNICAL NOTE 3804

A FACTOR AFFECTING TRANSONIC LEADING-EDGE FLOW SEPARATION

By George P. Wood and Paul B. Gooderum

SUMMARY

A change in flow pattern that was observed as the free-stream Mach number was increased in the vicinity of 0.8 was described in NACA Technical Note 1211 by Lindsey, Daley, and Humphreys. The flow on the upper surface behind the leading edge of an airfoil at an angle of attack changed abruptly from detached flow with an extensive region of separation to attached supersonic flow terminated by a shock wave. In the present paper, the consequences of shock-wave-boundary-layer interaction are proposed as a factor that may be important in determining the conditions under which the change in flow pattern occurs. When the Mach number is high enough, the attached-flow pattern exists because then the shock wave is far enough behind the leading edge to keep the influence of the high pressure behind the shock wave from extending through the boundary layer to the immediate vicinity of the leading edge and affecting the flow there. Some experimental evidence in support of the importance of shock-wave-boundary-layer interaction is presented.

INTRODUCTION

Observations of the change in the flow pattern near the leading edge of a wedge or other airfoil at an angle of attack as the subsonic free-stream Mach number was increased are reported by Lindsey and his coworkers in reference 1. This reference shows that, at the lower subsonic Mach numbers, an extensive region of separated flow exists on the upper surface, and that, as the Mach number is increased, the flow becomes attached more or less abruptly (within an increase of 0.05 or less in Mach number). Not only is this abrupt change in flow configuration an interesting phenomenon in itself, but there are also practical reasons for considering the cause of it. When the flow is detached, the instability of the flow may contribute to buffeting (ref. 2). When the flow attaches, there may be an undesirably abrupt change in the forces on the airfoil. Reference 1 infers that attachment of the flow occurs only when the height of the supersonic zone at the nose has become an appreciable fraction of the chord. The present paper proposes the consequences of shock-wave-boundary-layer interaction as a factor that may play a large role in determining when attachment occurs. Thus,

in more detail than previously, it relates the size of the supersonic zone, as specified by the location of the terminating shock wave, to the attachment phenomenon. Some experimental evidence of the importance of this factor is presented.

SYMBOLS

C_p	pressure coefficient, $\frac{p - p_\infty}{q_\infty}$
$C_{p,\max}$	maximum pressure coefficient, $\frac{p_{\max} - p_1}{q_1}$
d	upstream influence distance, ft
M	Mach number
p	pressure, lb/sq ft
p_{\max}	maximum pressure behind shock wave, lb/sq ft
q	dynamic pressure, $\frac{\rho V^2}{2}$, lb/sq ft
R	Reynolds number
r	radius of curvature of leading edge, ft
T	temperature, °R
V	velocity, ft/sec
x	distance along flat-plate surface of model from juncture of circular arc and straight section, ft
γ	ratio of specific heats
δ^*	boundary-layer displacement thickness, ft
θ	angular distance from center line, deg
μ	coefficient of viscosity, slugs/ft-sec
ρ	density, slugs/cu ft

Subscripts:

lam	laminar
t	total
turb	turbulent
l	ahead of base of shock wave
∞	free stream

APPARATUS

The blowdown jet that was used for the experiments was operated by dry, compressed air from storage tanks. The air passed through automatic pressure regulators, through a settling chamber, and then through a subsonic nozzle to the atmosphere. The top and the bottom of the test section were open to the atmosphere, and the sides were closed by straight extensions of the two sides of the nozzle. The sides of the test section contained glass windows of interferometer quality. The height of the test section was 6 inches, and the width was 4 inches. Interferograms were taken with a Mach-Zehnder interferometer that is described in reference 3. The duration of the light source was about 3 microseconds. The interferometer was so adjusted that the interference fringes were not contours of constant density, but the density at any location could be determined from the fringe shift at that location (as in ref. 3).

The model was a 5/16-inch-thick flat plate with a semicircular leading edge and a chord of 3 inches. It completely spanned the test section except for a 1/16-inch gap at each end. The model was supported by two struts on the lower surface. The struts were rigid enough to prevent any observable lateral vibration (change in end clearance) from occurring during a run. (Vibration with an amplitude of as much as about 0.001 inch would have been observed.) The model was instrumented with three static-pressure orifices in the rounded leading edge and seven in the straight section immediately behind the leading edge. The orifices were spaced about 0.1 inch apart in a chordwise direction and about 0.24 inch apart in a spanwise direction.

The model was placed at an angle of attack of 4°. The range of Mach number was from 0.56 to 0.88. The range of Reynolds number, based on free-stream conditions, was from about 5×10^6 per foot at the lowest Mach number to about 8×10^6 per foot at the highest Mach number.

The free-stream Mach numbers given herein were calculated from the ratio of measured stagnation pressure in the settling chamber to measured atmospheric pressure under the assumption, which is not strictly true, that free-stream pressure was equal to atmospheric pressure. The use of as many as three significant figures in Mach number is merely a means of indicating relative Mach numbers.

The turbulence level in the empty test section was not measured, but measurements on other somewhat similar blowdown jets showed the level to be high in them.

For some of the interferograms (described subsequently), earlier transition of the boundary layer was presumably induced by a 0.02-inch-diameter wire that was stretched across the test section about 1 inch ahead of the model and about 1/8 inch below the center line, extended, of the model.

RESULTS AND DISCUSSION

Description of Change in Flow Pattern

The change in the flow pattern that is discussed herein is illustrated by the interferograms of figure 1, which show the flow in the vicinity of the leading edge of the model at an angle of attack of 4° . Figures 1(a) to 1(g) show an extensive separated region on the upper surface, and figures 1(h) to 1(l) show that the separated region has been replaced by attached supersonic flow that is followed by a nearly normal shock wave. The Mach number gap between the two flow patterns in figures 1(g) and 1(h) is seen to be only 0.006. (The attention of those readers who are not familiar enough with interferograms to recognize the various features of the flow by inspection of an interferogram is directed to figure 2, where the fringe configurations characteristic of various features of the flow are pointed out.)

Figure 3 shows the pressure distribution, obtained by analysis of the interferograms, on the curved portion of the model at four Mach numbers for which the detached-flow pattern exists and at one for which the attached-flow pattern exists. Figure 4 shows the pressure distribution, obtained from the pressure orifices, on the straight portion of the model at five Mach numbers for which the flow is attached, and also repeats from figure 3 the pressure distribution on the curved portion for one of these.

In order to determine whether there was any hysteresis in the attachment-detachment process, very slow and careful changes in the Mach number of the flow were made while the manometers connected to the

orifices in the airfoil were observed. It was found that, as the free-stream Mach number was increased, the flow usually attached at a Mach number of 0.835, but sometimes it attached at 0.834 or 0.833. As the Mach number was decreased, the flow always detached at a Mach number of 0.829. Thus, a small amount of hysteresis was observed.

Shock-Wave-Boundary-Layer Interaction as a Factor

in Flow-Pattern Change

In the present section, shock-wave-boundary-layer interaction is proposed as an important factor in the observed change in flow pattern. In order to describe the proposed influence of this factor, it is advisable first to consider in some detail the flow about the model used in the present experiments. In an incompressible, inviscid fluid, the flow on the upper surface of the model, in going around the curved leading edge, would be expected to accelerate from the stagnation point to some location that is approximately 90° from the stagnation point and to decelerate rearward of that location. In a compressible, viscous fluid, at free-stream Mach numbers low enough to cause the flow to be everywhere subsonic, the adverse pressure gradient that is associated with the deceleration of the subsonic flow would be expected to be large enough to cause separation of the laminar boundary layer in the vicinity of the 80° station, just as it does on a circular cylinder. (See ref. 4, fig. 218.) As the free-stream Mach number was increased in the present experiments, a supersonic zone, embedded in the subsonic flow, developed on the curved portion of the model. This zone increased in size as the free-stream Mach number was increased further. At a free-stream Mach number of 0.812, for example, for which the flow is sonic at $C_p = -0.40$, the supersonic zone began at about the 57° station, as can be determined from figure 3, and extended rearward for about two model thicknesses, where it was terminated by a shock wave, as can be seen from figure 1(f). The flow, however, remained separated at this Mach number.

When the Mach number was high enough, however, the detached flow attached to the surface. What is proposed in the present paper is that, when the free-stream Mach number is high enough, the attached-flow configuration occurs because then the terminating shock wave is far enough back that the influence of the high pressure behind it is not propagated far enough forward through the boundary layer to influence the flow on the curved portion of the model. Conversely, when the Mach number is lower, the pattern of attached flow cannot occur because the shock wave is far enough forward that the influence of the high pressure behind it extends far enough forward to cause separation of the boundary layer in the vicinity of the 80° station.

When the Mach number becomes "high enough" depends on the state of the boundary layer, in the sense that the distance of upstream influence of the high pressure behind a shock wave depends on the Reynolds number, the local Mach number, the pressure ratio across the shock wave, and whether the boundary layer is laminar or turbulent. The distance is several times greater for a laminar than for a turbulent boundary layer, other factors being equal. It is believed that, for the conditions of the present experiments, the attached-flow configuration occurs only when the shock wave can be located downstream of the transition from a laminar to a turbulent boundary layer on the surface. When the shock wave interacts with a turbulent boundary layer, its upstream distance of influence is small and, on the present model, does not extend far enough forward to cause separation of the flow on the curved portion of the model.

Supporting Evidence

Supporting evidence for the importance of shock-wave-boundary-layer interaction as a factor in the attachment-detachment process would presumably be obtained if it could be shown that, when the boundary layer is made turbulent artificially, the shock wave can be brought nearer to the leading edge (at Mach numbers less than 0.835) without having separation occur on the curved portion of the model. Figure 5 shows the flow pattern obtained at the lower Mach numbers with a 0.02-inch-diameter wire stretched across the test section about 1 inch ahead of the model. With the boundary layer thus probably made turbulent closer to the stagnation point, the shock wave is seen to be located closer to the leading edge than without the wire. The free-stream Mach number can be reduced to 0.751 (fig. 5(d)) without having the flow detach. To ascertain whether the wire produced any significant difference in the flow around the model other than in the boundary layer, the pressure distribution on the model at a free-stream Mach number of 0.83 was measured both with and without the wire and was found to be only slightly changed by the presence of the wire, as is shown by figure 6.

It might also be mentioned that, if transition occurs just ahead of the shock wave in figure 1(h), the Reynolds number of transition based on free-stream conditions is then about 3×10^5 . This value compares with the Reynolds number of transition in wind tunnels that have an "average" amount of free-stream turbulence, which figure 4 of reference 5 shows to be about 5×10^5 . (Fig. 1 of ref. 5 shows that the Reynolds number of transition as a function of intensity of free-stream turbulence can range between the rather wide limits of 10^5 and 3×10^6 . It should, perhaps, be pointed out that in the present experiments the flow along the surface had experienced both a falling and a rising pressure before reaching what is believed to be the location of transition.)

It is also of interest to obtain, from the present experiments and the proposed interpretation of them, the upstream distance of influence of the high pressure behind the shock wave for both laminar and turbulent boundary layers and to compare these distances with those reported, for example, in reference 6 by Gadd, Holder, and Regan. Reference 6 reports a detailed experimental investigation of shock-wave-boundary-layer interaction on a flat plate, including measurements of the upstream distance through which the pressure and the boundary layer are affected. The results, however, cannot be expected to be exactly comparable to the present results.

In the experiments of reference 6 the shock wave was generated by two means, and different values of the upstream distance were obtained in the two cases. In one case a wedge in the stream produced a shock wave that interacted with the boundary layer on a plate, and in the other case a wedge held in contact with the plate produced a shock wave. In the present experiments the shock wave was generated in a way different from either of these. Furthermore, instead of a uniform free-stream flow along the flat plate, as in the experiments of reference 6, there is in the present case a pressure gradient in the flow along the plate due to reflections from the sonic line.

A determination of the distances ahead of the shock wave through which the high pressure affected both the laminar and the turbulent boundary layer can be made by use of the interferogram for a free-stream Mach number of 0.835, figure 1(h) (or by use of the pressure distribution on the model, fig. 4). Expansion waves that originate at the curve of the leading edge are reflected from the sonic line as compression waves and again from the surface as compression waves, and they produce a positive pressure gradient along the flat surface, as shown in figure 4. The pressure gradient is evidenced by the oblique orientation of the interference fringes in the supersonic region in figure 1(h). Just ahead of the shock wave, however, the fringes are more closely spaced, and thus indicate a greater pressure gradient. The extent along the surface of these closely spaced fringes is taken as the distance ahead of the shock wave that the boundary layer is affected by the pressure behind the shock wave. To conform with one of the definitions of "upstream influence distance" used in reference 6, the distance is taken as that from the beginning of the closely spaced fringes to where the rear plane of the shock wave extrapolated would intersect the surface. The distance, as measured on figure 1(h), is about 0.019 foot. It is assumed, herein, that throughout this distance the boundary layer is turbulent. There can be little doubt about the correctness of the assumption that the shock wave is interacting with a turbulent boundary layer. Experience confirms that the pattern shown in figure 1(h) occurs when the boundary layer is turbulent but does not occur when it is laminar. Furthermore, comparison of the form of the variation of pressure, as shown by the variation of C_p in figure 4, with the forms of the pressure variation

shown in figures 13, 14, 20, and 21 of reference 6 shows similarity between the form of variation in figure 4 and that obtained when the boundary layer is turbulent.

If the aforementioned idea of the present paper is correct, that the change in flow pattern that occurs at a Mach number just slightly less than that of figure 1(h) is a result of interaction of the shock wave with a laminar boundary layer, then it follows that the point of farthest upstream extent of the region of shock-wave-boundary-layer interaction in figure 1(h), which is at $x = 0.044$ foot, is also approximately the farthest upstream extent of the turbulent boundary layer. As a rough approximation, therefore, the distance from that position to the beginning of the straight section can be taken as the upstream influence distance for a laminar boundary layer. This distance is accordingly 0.044 foot. This reasoning ignores any finite extent of the transition region and also the fact that the rear of the shock wave would not move as far forward as $x = 0.044$ foot if the Mach number were reduced from 0.835 to 0.829.

A comparison of the present results on upstream distance of influence with those of reference 6 is shown in figures 7 to 10. (Calculations of Mach number, Reynolds number, maximum pressure coefficient, and boundary-layer thickness are given in the appendix.) Figures 7 and 8, for laminar boundary layers, were taken from figures 16 and 17 of reference 6, and a point, shown by the circle, was added to represent the result of the present investigation. (The Mach number ahead of the base of the shock wave is 1.5.) Figures 9 and 10, for turbulent boundary layers, were taken from figures 23 and 24 of reference 6, and again the result of the present investigation is shown by the circle.

The comparison shows at least an order-of-magnitude agreement. Very good agreement was not expected because of differences in the methods of generating the shock wave. In the laminar case, where the present result for distance of influence is a shorter distance than was expected from the results of reference 6, much of the difference may well be due to the shock wave's being too close to the leading edge of the model for the full distance of upstream influence to be developed.

CONCLUDING REMARK

This paper proposes that shock-wave-boundary-layer interaction is a factor that may be important in determining the Mach number at which

the flow becomes attached to the upper surface of an airfoil at a positive angle of attack and presents some experimental evidence to support this idea.

Langley Aeronautical Laboratory,
National Advisory Committee for Aeronautics,
Langley Field, Va., June 18, 1956.

APPENDIX

DATA FOR FIGURE 1(h)

In this appendix, calculations are made of Reynolds number, boundary-layer thickness, local Mach number, and so forth, for the flow shown in figure 1(h).

The free-stream conditions are:

p_t , lb/sq ft	3,410
T_t , °R	533
ρ_t , slugs/cu ft	0.00369
p_∞ , lb/sq ft	2,160
ρ_∞ , slugs/cu ft	0.00266
T_∞ , °R	467
M_∞	0.835
V_∞ , ft/sec	883
μ_∞ , slugs/ft-sec	3.36×10^{-7}

The radius of curvature of the leading edge r is 0.013 foot.

The Reynolds number per foot R/x based on free-stream conditions is 7×10^6 .

First, the boundary-layer thickness at the stagnation point is calculated. According to reference 7, the boundary-layer thickness δ^* at the stagnation point of a circular cylinder is

$$\delta^* = 0.64 \left(\frac{\rho}{\mu} \frac{dV}{dx} \right)^{-1/2}$$

and

$$\frac{dV}{dx} = \frac{2V_\infty}{r}$$

Therefore, $\frac{dV}{dx}$ is 136,000 ft/sec-ft and δ^* is 0.20×10^{-4} foot.

It is assumed that the boundary layer does not thicken appreciably along the curved portion of the model because of the large negative pressure gradient. If the positive pressure gradient along the straight section is ignored, then the boundary-layer thickness can be calculated, as was done in reference 6, from the equation

$$\delta^* = 1.72 \left(1 + 0.277M^2\right) \frac{x}{\sqrt{R}}$$

As obtained from the measured pressures, the Mach number at the beginning of the straight section is 1.78, and at the beginning of the upstream influence of the shock wave it is 1.52. For use in the preceding equation, an average value of 1.65 is taken. The distance along the straight section to the beginning of the upstream influence is 0.044 foot. The value of ρV for a Mach number of 1.65 is 0.79 times its value for a Mach number of 0.83. Therefore, the value of the Reynolds number based on ambient rather than on free-stream conditions is $7.0 \times 10^6 \times 0.79 \times 0.044$, or 2.43×10^5 and δ^* is 2.7×10^{-4} foot. On addition of the thickness at the stagnation point, δ^* becomes 2.9×10^{-4} foot. As a very rough approximation, with consideration of figure 41(a) of reference 7, it is assumed that the pressure gradient increases the thickness by one-third. Then δ_{lam}^* is 3.9×10^{-4} foot.

For calculating the displacement thickness of the turbulent boundary layer, essentially the same procedure is followed as was used in reference 6. The momentum thickness of the laminar boundary layer at transition is calculated from the displacement thickness, the assumption being made that transition does not affect the value of the momentum thickness, the effective origin of the turbulent boundary layer is calculated from the momentum thickness, and the displacement thickness of the turbulent boundary layer is calculated from the equation used in reference 6:

$$\delta_{turb}^* = 4.75 \times 10^{-2} \frac{x_{turb}}{R_{turb}^{0.2}} \frac{1 + 0.35M^2}{\left(1 + 0.88 \frac{\gamma - 1}{2} M^2\right)^{0.44}}$$

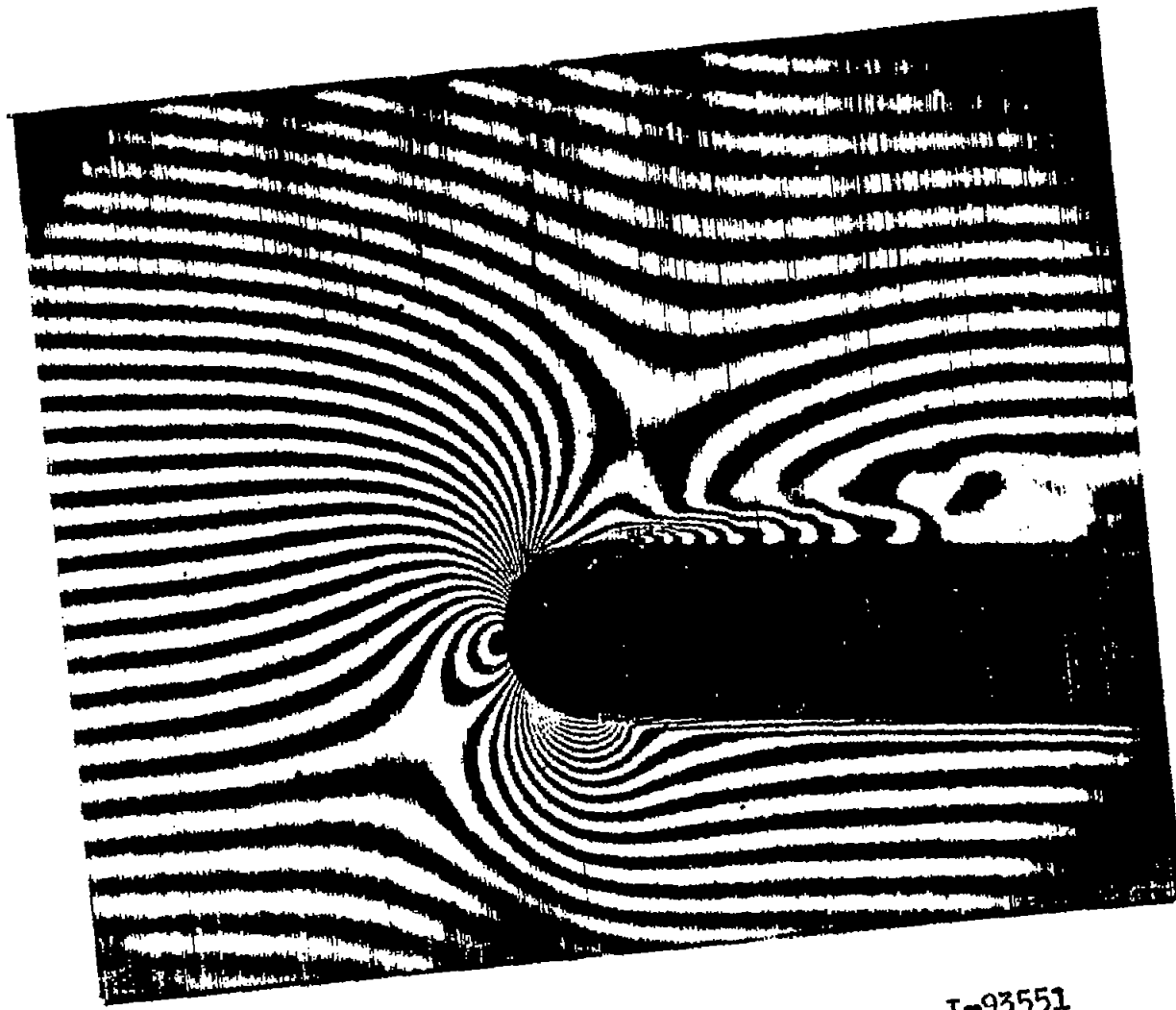
The resulting value of δ_{turb}^* is 2.6×10^{-4} foot.

For use in comparing the present results with those of reference 6, the maximum pressure behind the shock wave is needed. The Mach number at the beginning of the upstream influence of the shock wave is 1.52. The shock-wave angle near the foot of the shock wave is approximately 60° .

The theoretical value of the pressure ratio across the shock wave is 1.87. The highest ratio of pressure on the surface to pressure ahead of the shock wave, measured with the orifices, was 1.9. The pressure orifices, however, did not extend far enough rearward to indicate the maximum pressure. The value obtained by analysis of the interferogram was 2.2, and that value was used to calculate the maximum pressure coefficient as 0.74.

REFERENCES

1. Lindsey, W. F., Daley, Bernard N., and Humphreys, Milton D.: The Flow and Force Characteristics of Supersonic Airfoils at High Subsonic Speeds. NACA TN 1211, 1947.
2. Humphreys, Milton D.: Pressure Pulsations on Rigid Airfoils at Transonic Speeds. NACA RM L51L12, 1951.
3. Gooderum, Paul B., Wood, George P., and Brevoort, Maurice J.: Investigation With an Interferometer of the Turbulent Mixing of a Free Supersonic Jet. NACA Rep. 963, 1950. (Supersedes NACA TN 1857.)
4. Mair, W. A., and Beavan, J. A.: Flow Past Aerofoils and Cylinders. Vol. II of Modern Developments in Fluid Dynamics - High Speed Flow, ch. XIII, L. Howarth, ed., The Clarendon Press (Oxford), 1953, pp. 612-687.
5. Gazley, Carl, Jr.: Boundary-Layer Stability and Transition in Subsonic and Supersonic Flow. A Review of Available Information With New Data in the Supersonic Range. Jour. Aero. Sci., vol. 20, no. 1, Jan. 1953, pp. 19-28.
6. Gadd, G. E., Holder, D. W., and Regan, J. D.: An Experimental Investigation of the Interaction Between Shock Waves and Boundary Layers. Proc. Roy. Soc. (London), ser. A, vol. 226, no. 1165, Nov. 9, 1954, pp. 227-253.
7. Schlichting, H.: Lecture Series "Boundary Layer Theory." Part I - Laminar Flows. NACA TM 1217, 1949.

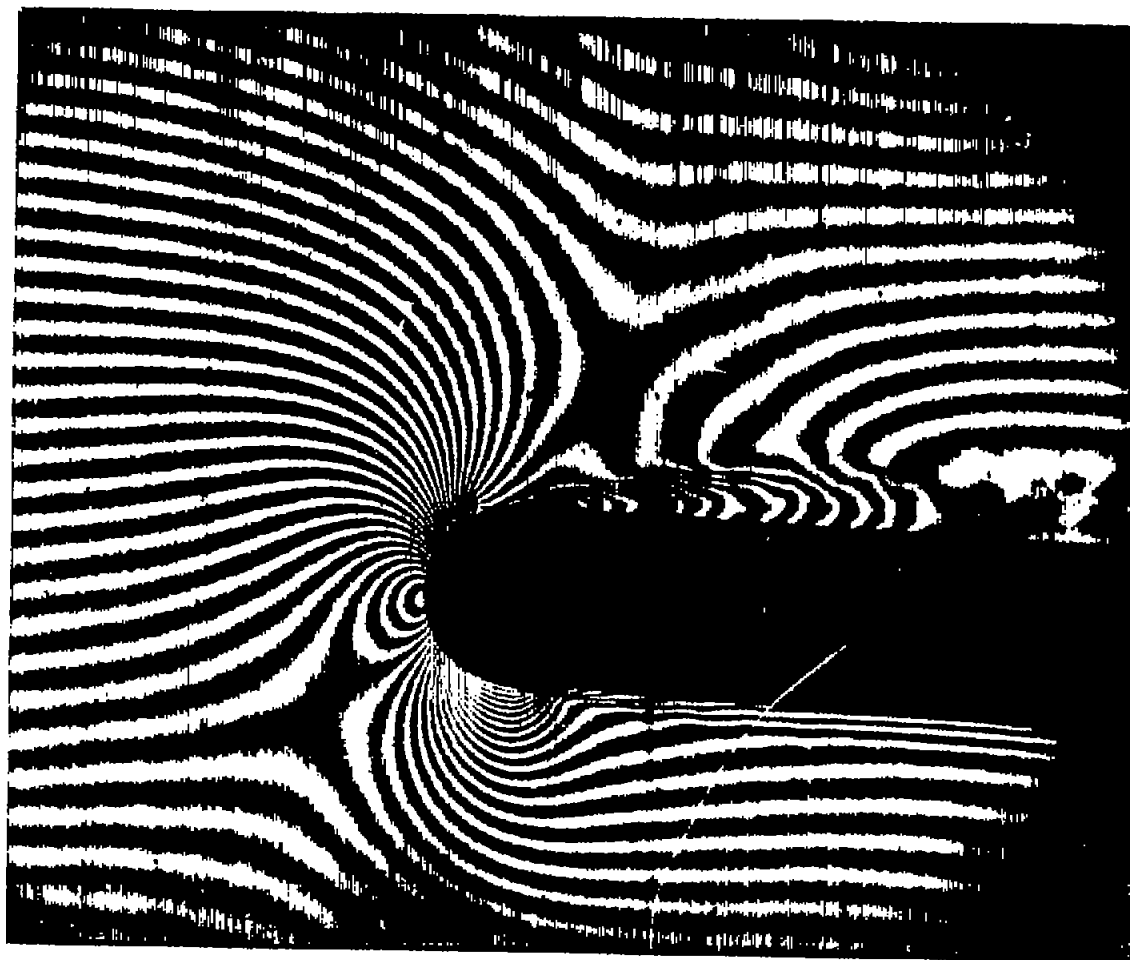


L-93551

(a) $M_{\infty} = 0.562$.

Figure 1.- Interferograms of the flow in the vicinity of the rounded leading edge of a flat plate $5/16$ inch thick. Angle of attack, 4° .

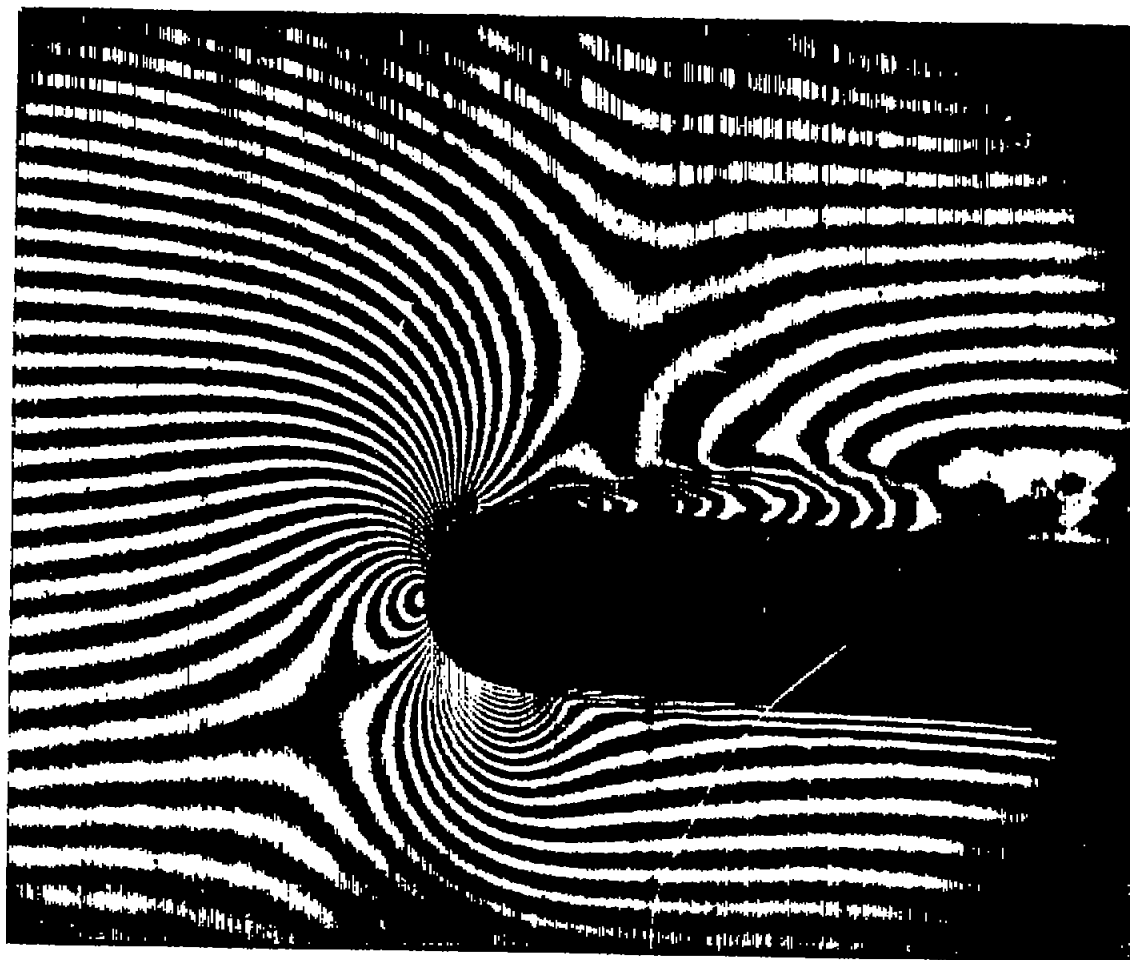
NACA TN 3804



(b) $M_{\infty} = 0.631.$

I-93552

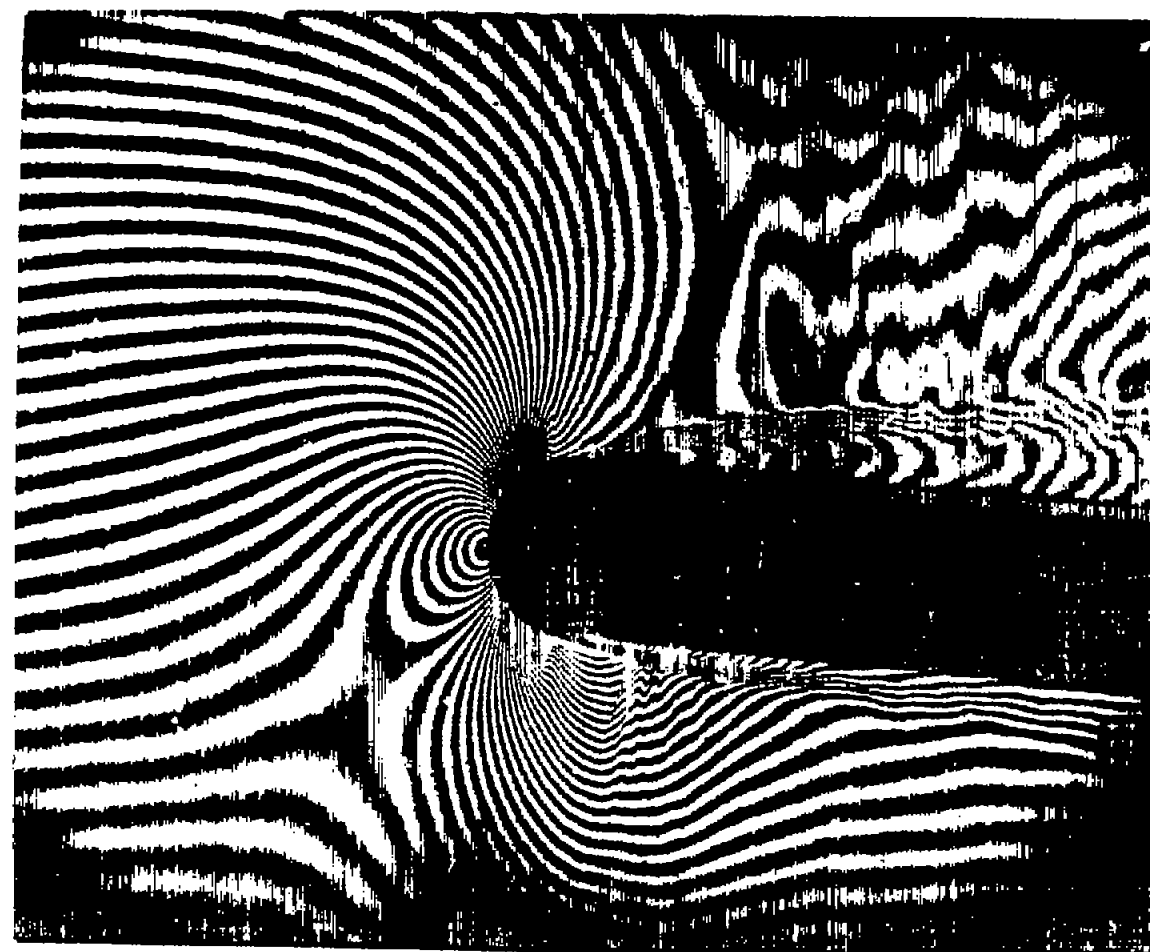
Figure 1.- Continued.



(b) $M_\infty = 0.631.$

I-93552

Figure 1.- Continued.

(d) $M_\infty = 0.763$.

I-93554

Figure 1.- Continued.

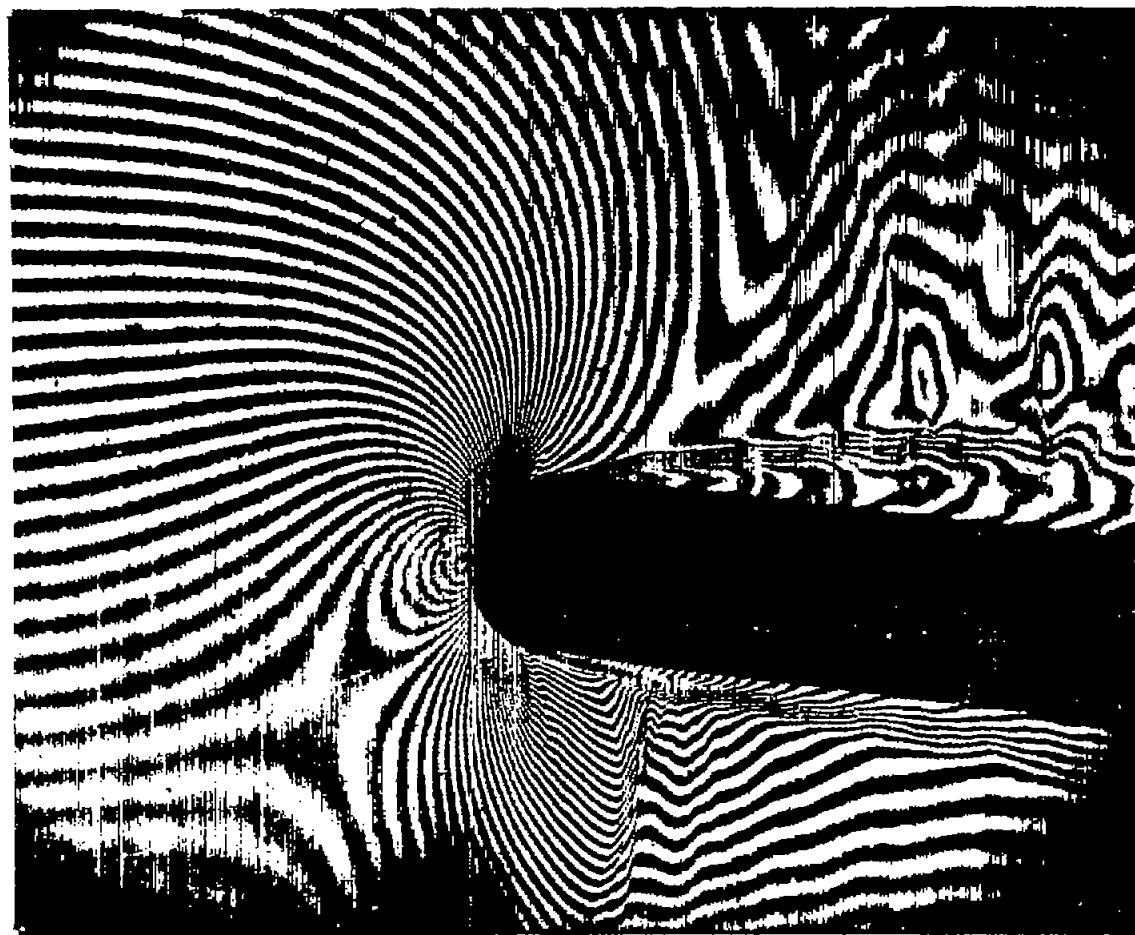
(e) $M_{\infty} = 0.799.$ **L-93555**

Figure 1.- Continued.

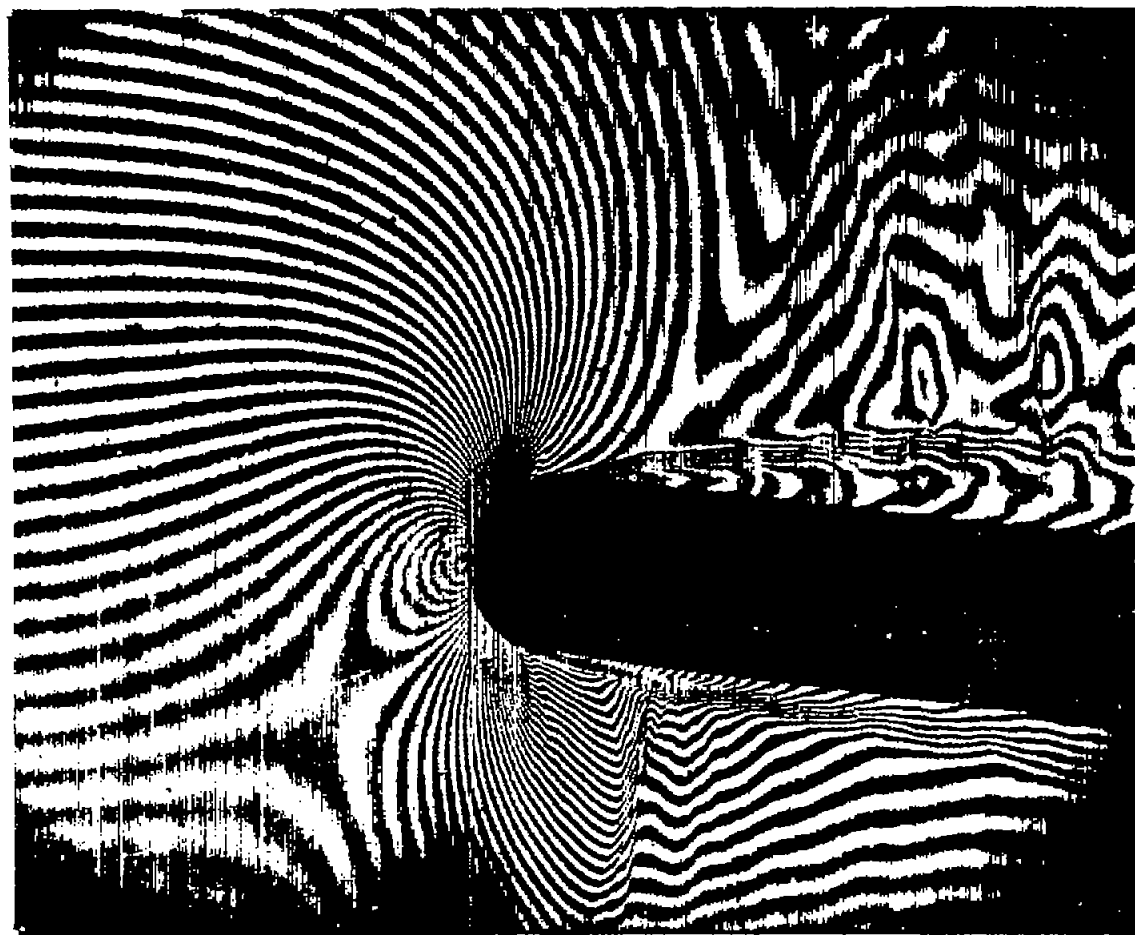
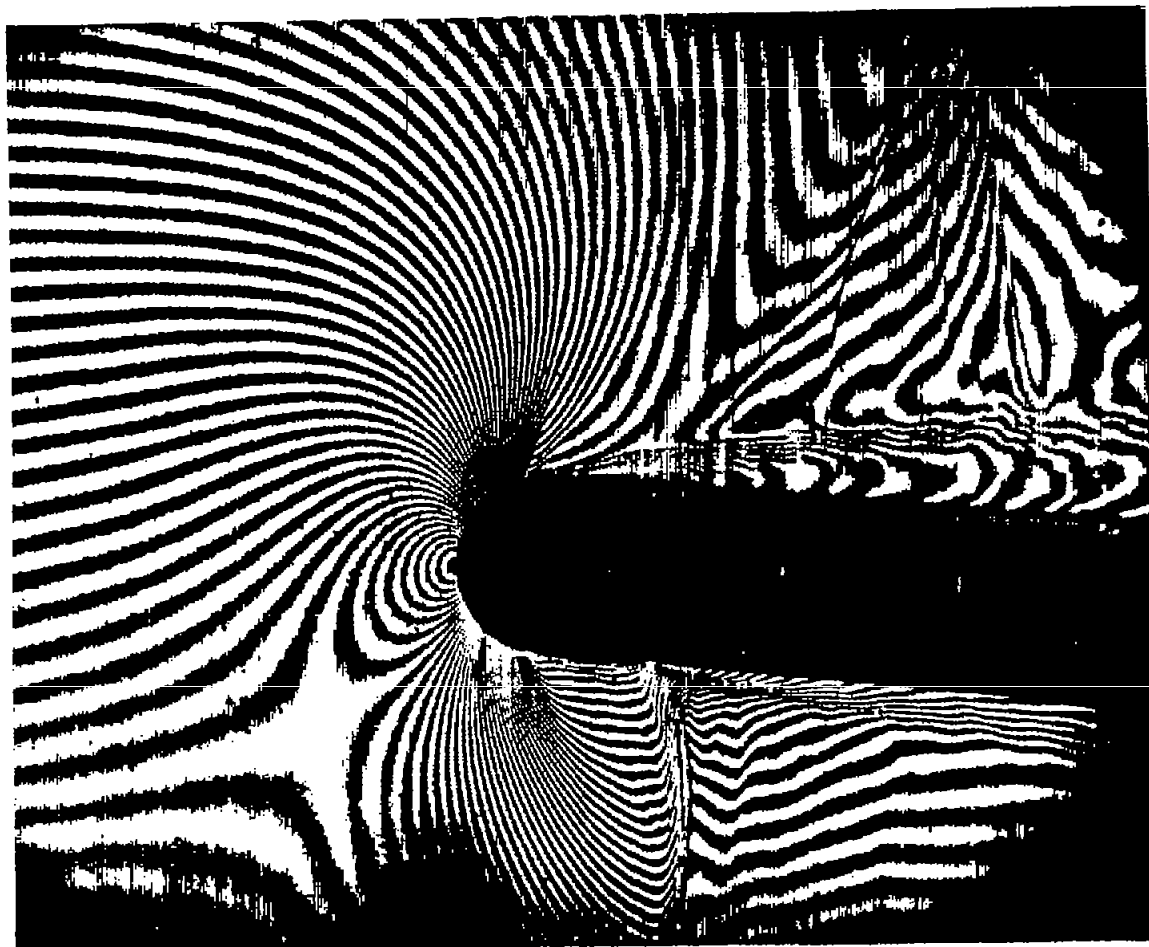
(e) $M_{\infty} = 0.799.$ **L-93555**

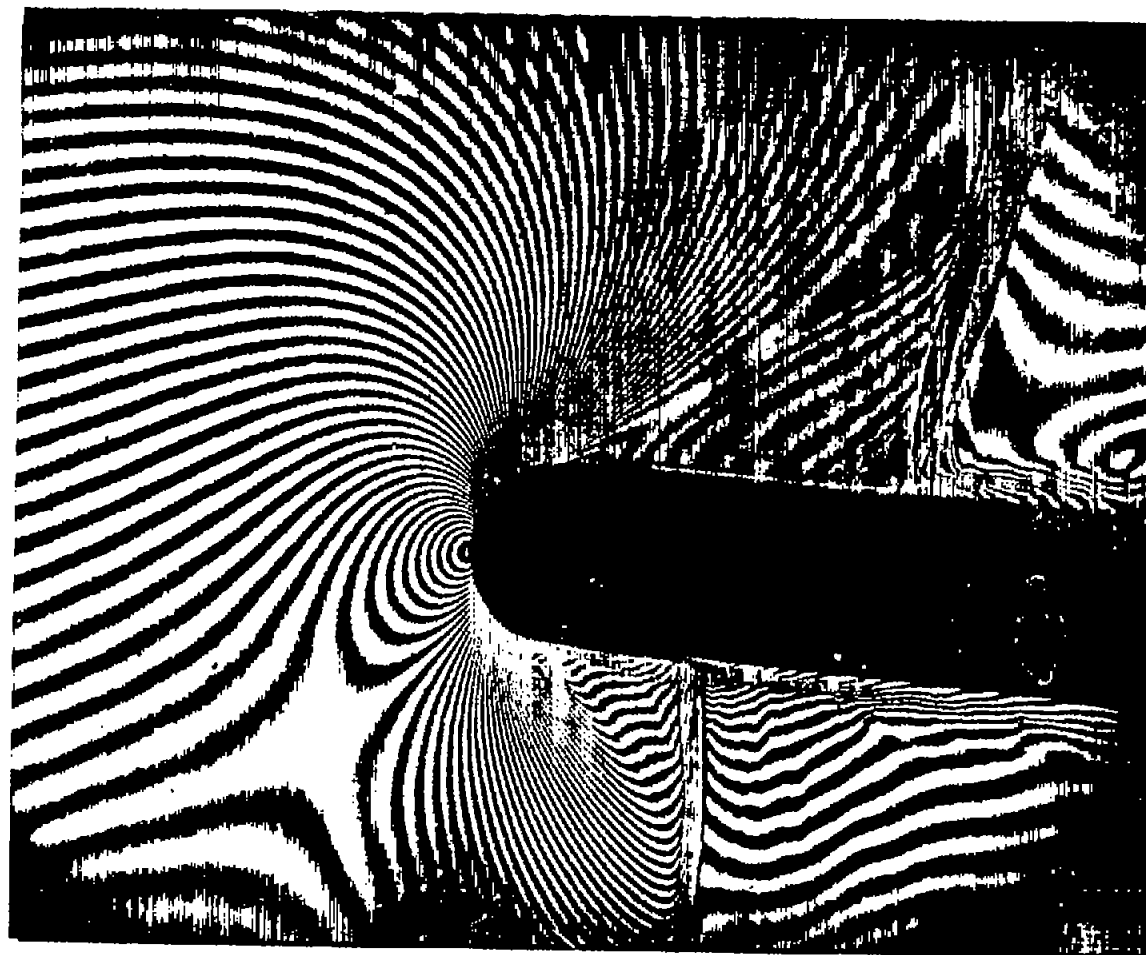
Figure 1.- Continued.



(g) $M_{\infty} = 0.829.$

L-93557

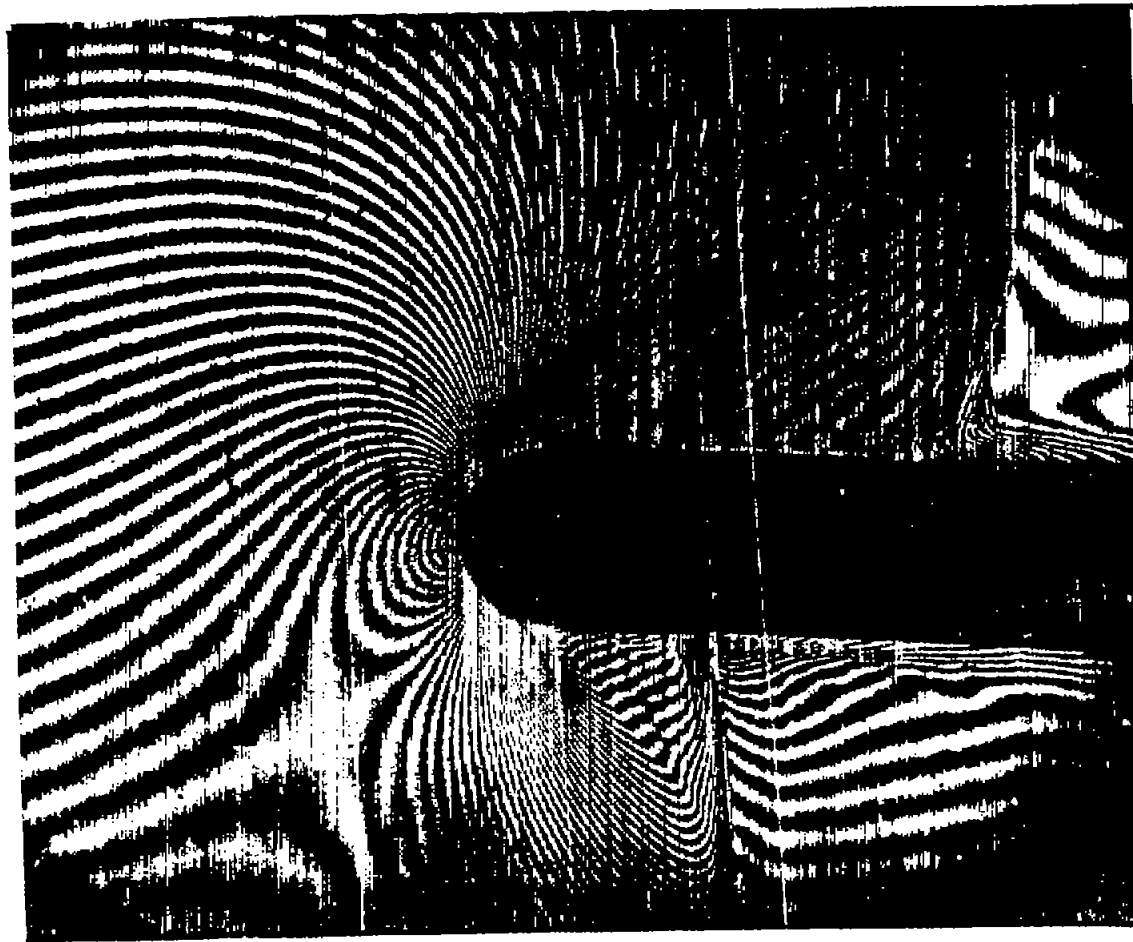
Figure 1.- Continued.



(h) $M_{\infty} = 0.835.$

I-93558

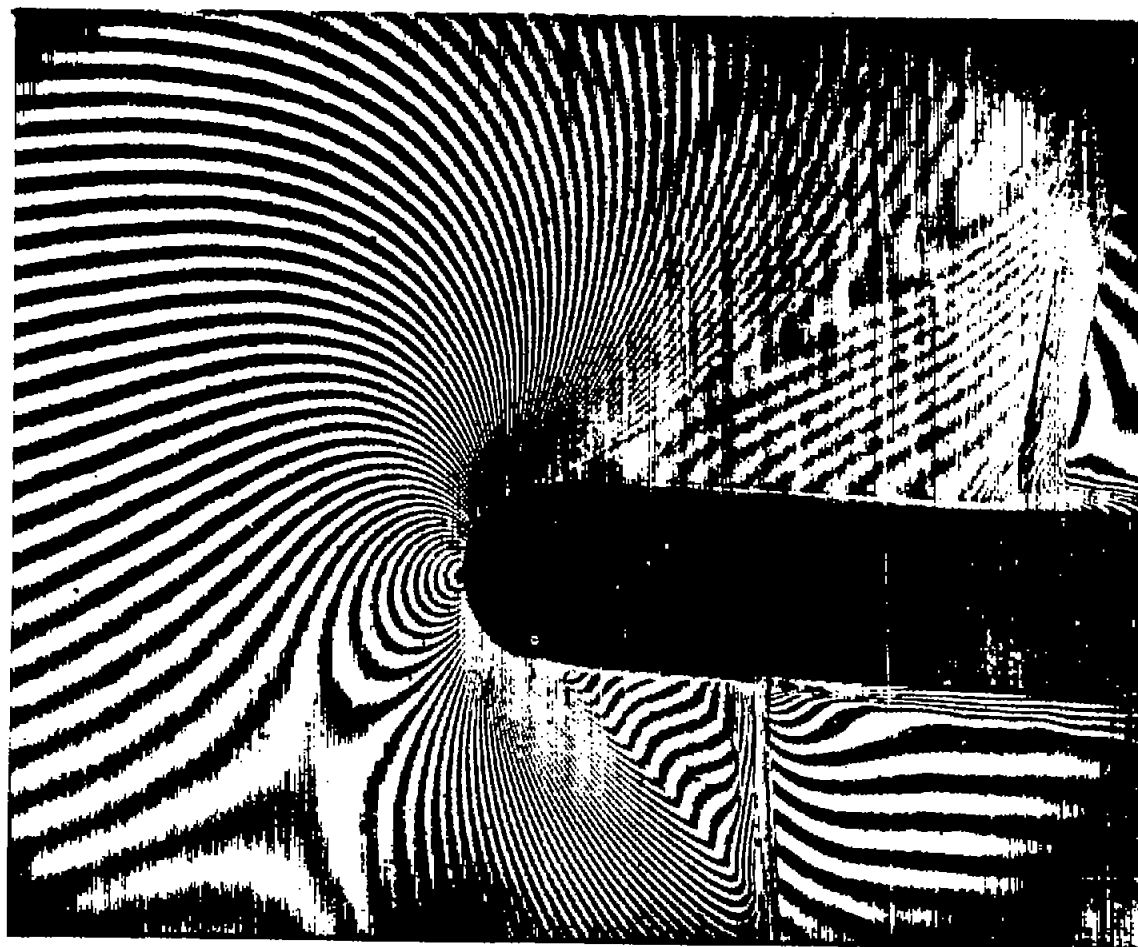
Figure 1.- Continued.



(i) $M_{\infty} = 0.847.$

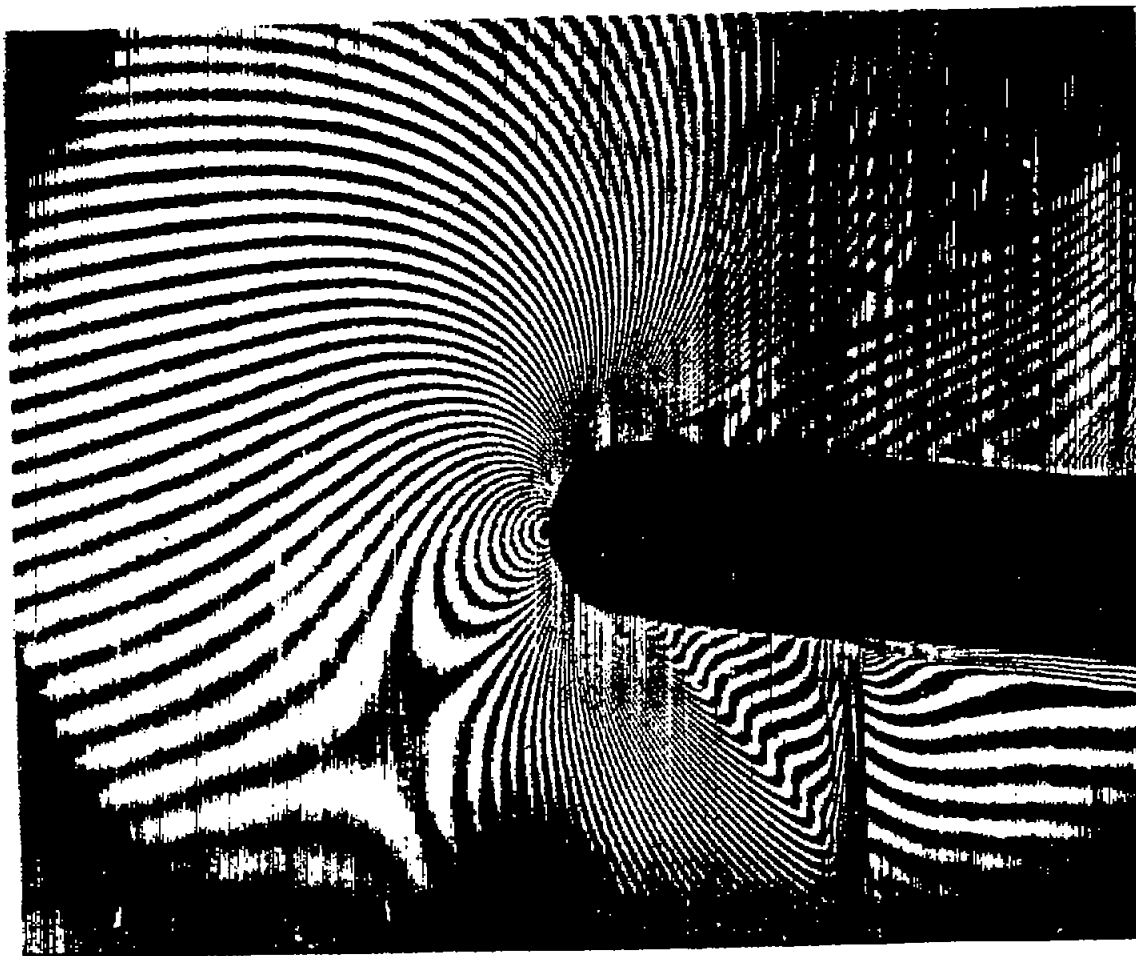
I-93559

Figure 1.- Continued.



(j) $M_\infty = 0.862.$ I-93560

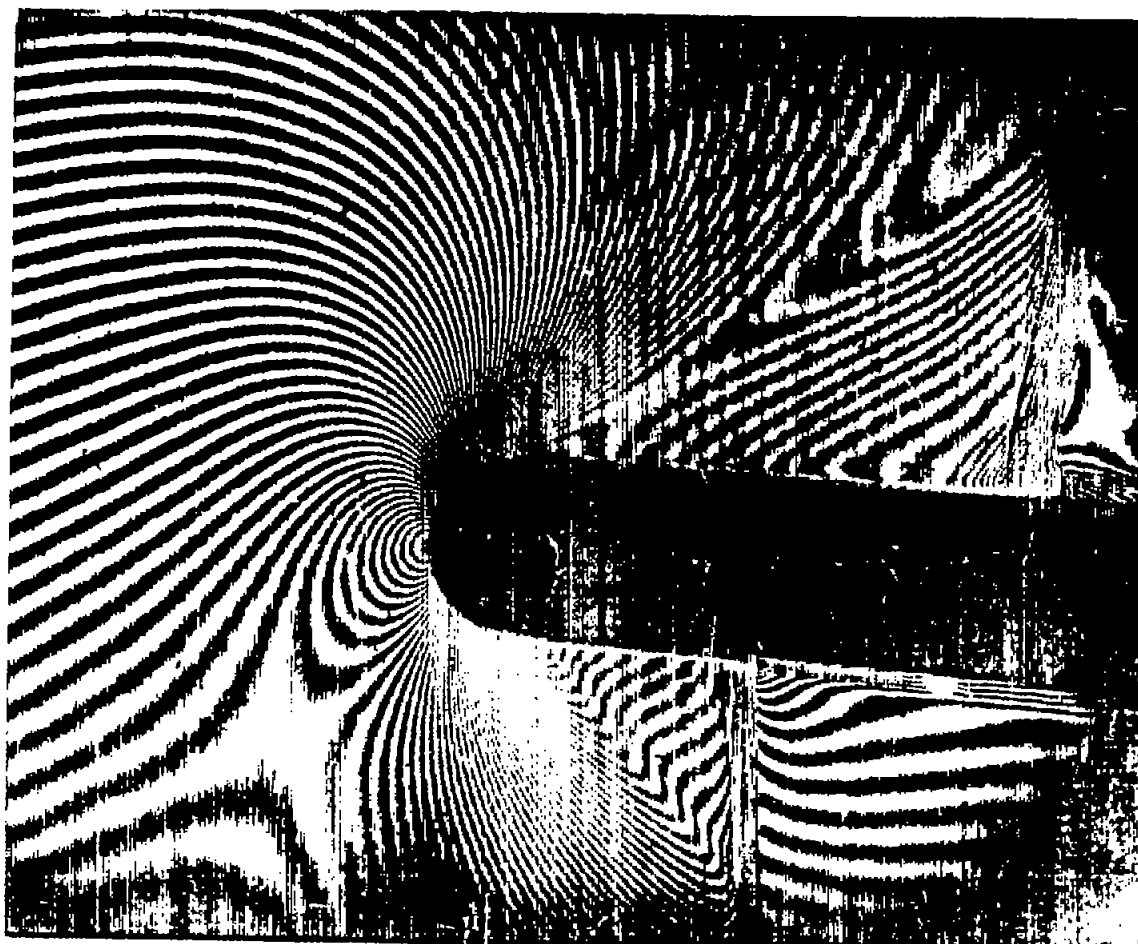
Figure 1.- Continued.



(k) $M_\infty = 0.867.$

L-93561

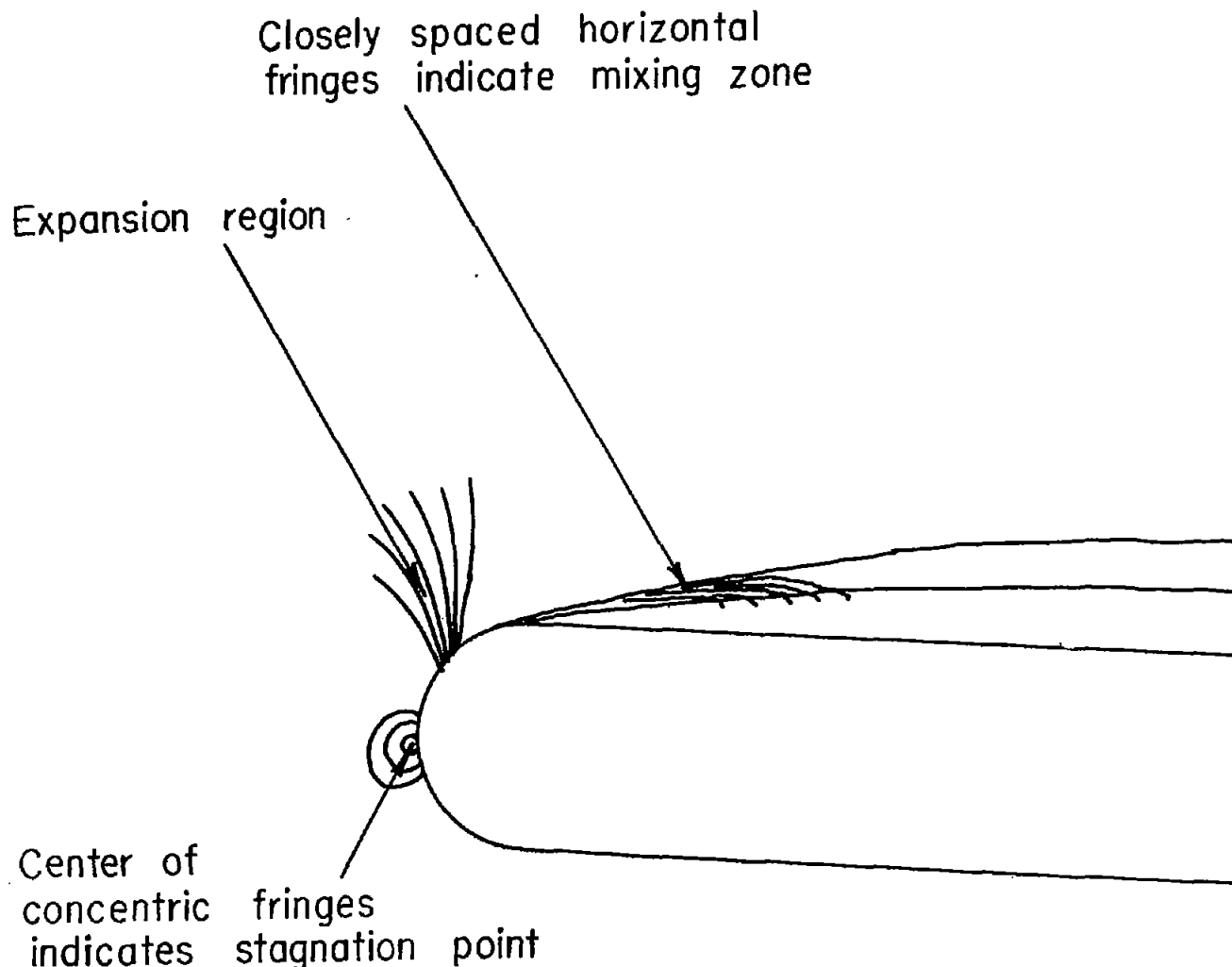
Figure 1.- Continued.



(1) $M_{\infty} = 0.877.$

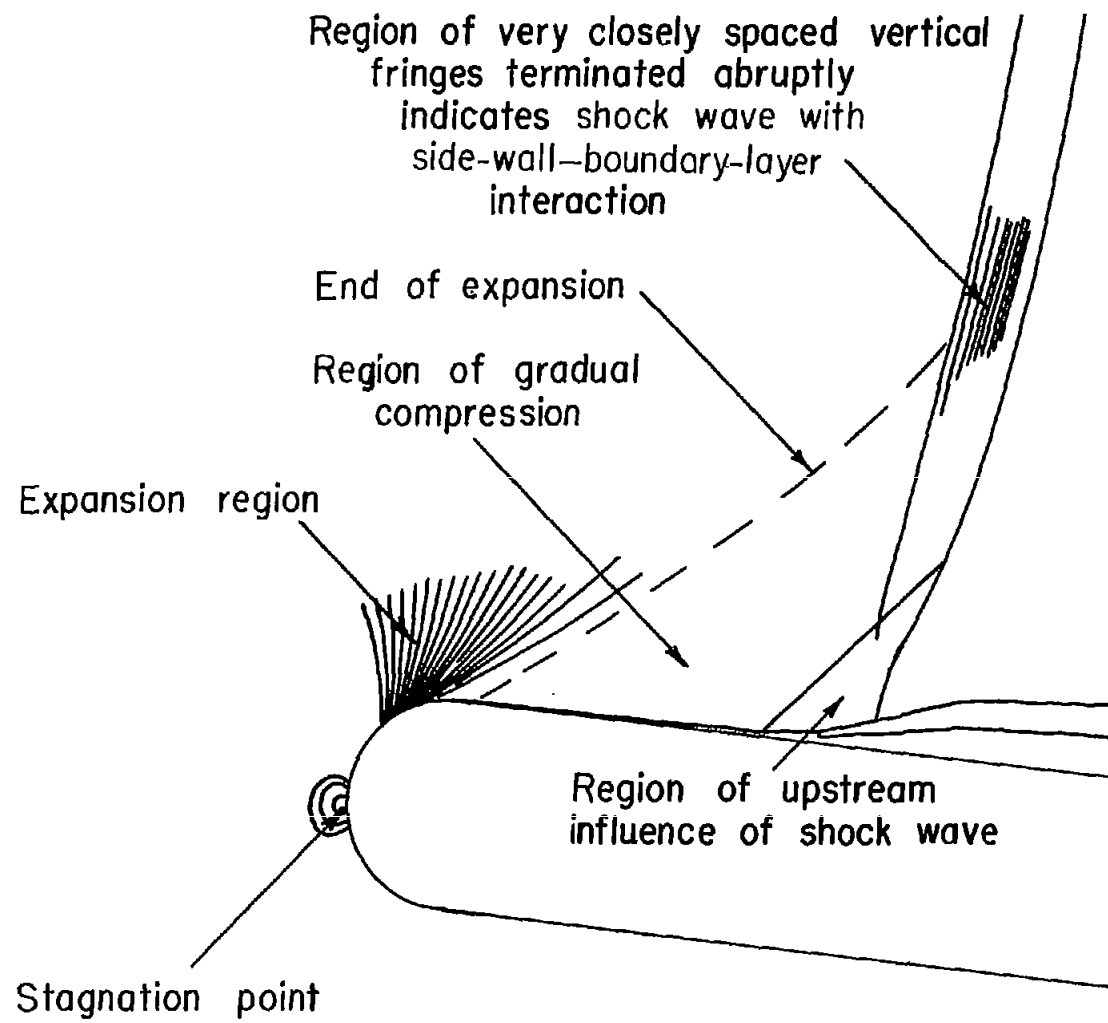
I-93562

Figure 1.- Concluded.



(a) Separated-flow pattern.

Figure 2.- Identification of various features of the flow.



(b) Attached-flow pattern.

Figure 2.- Concluded.

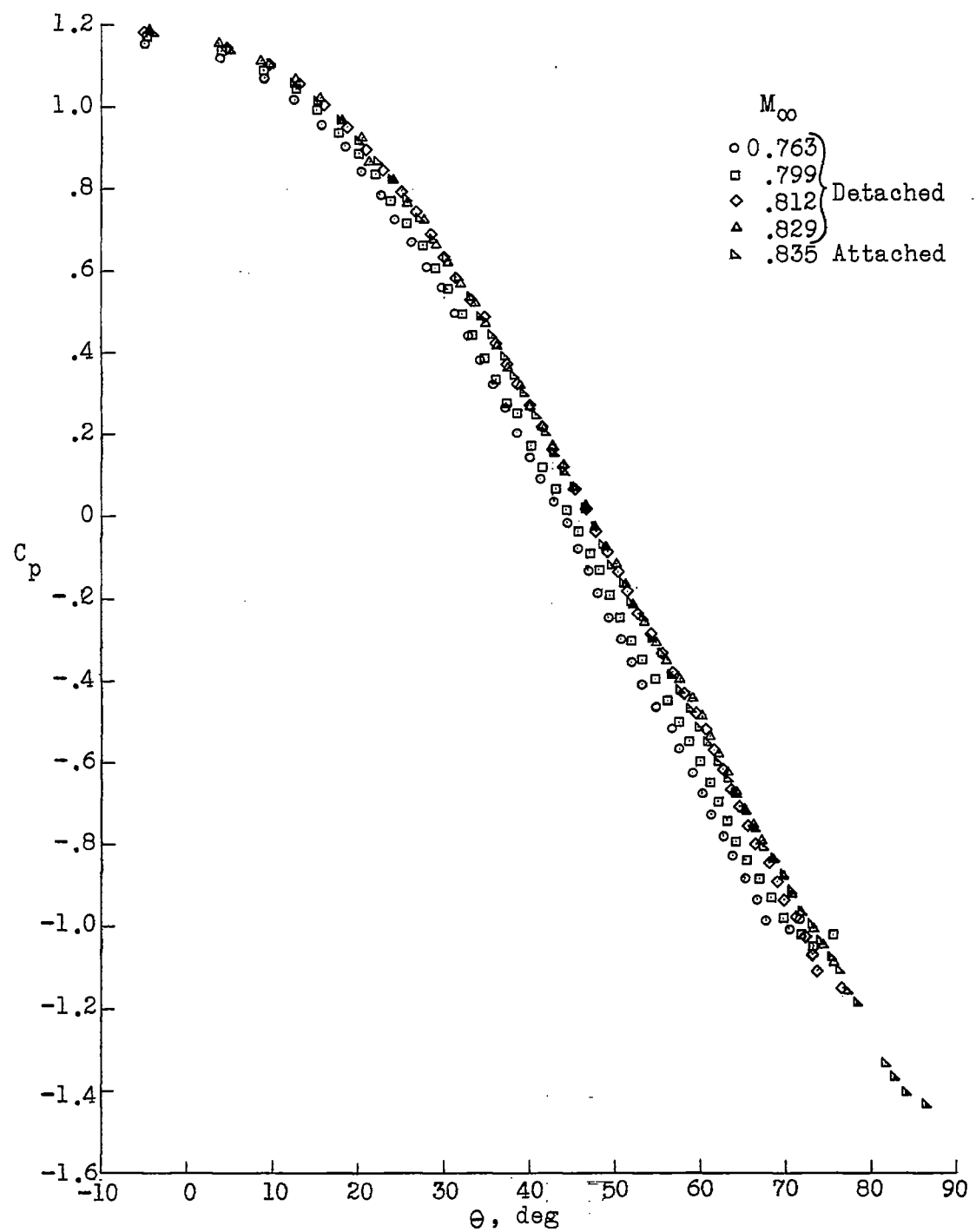


Figure 3.- Pressure distribution on curved portion of model.

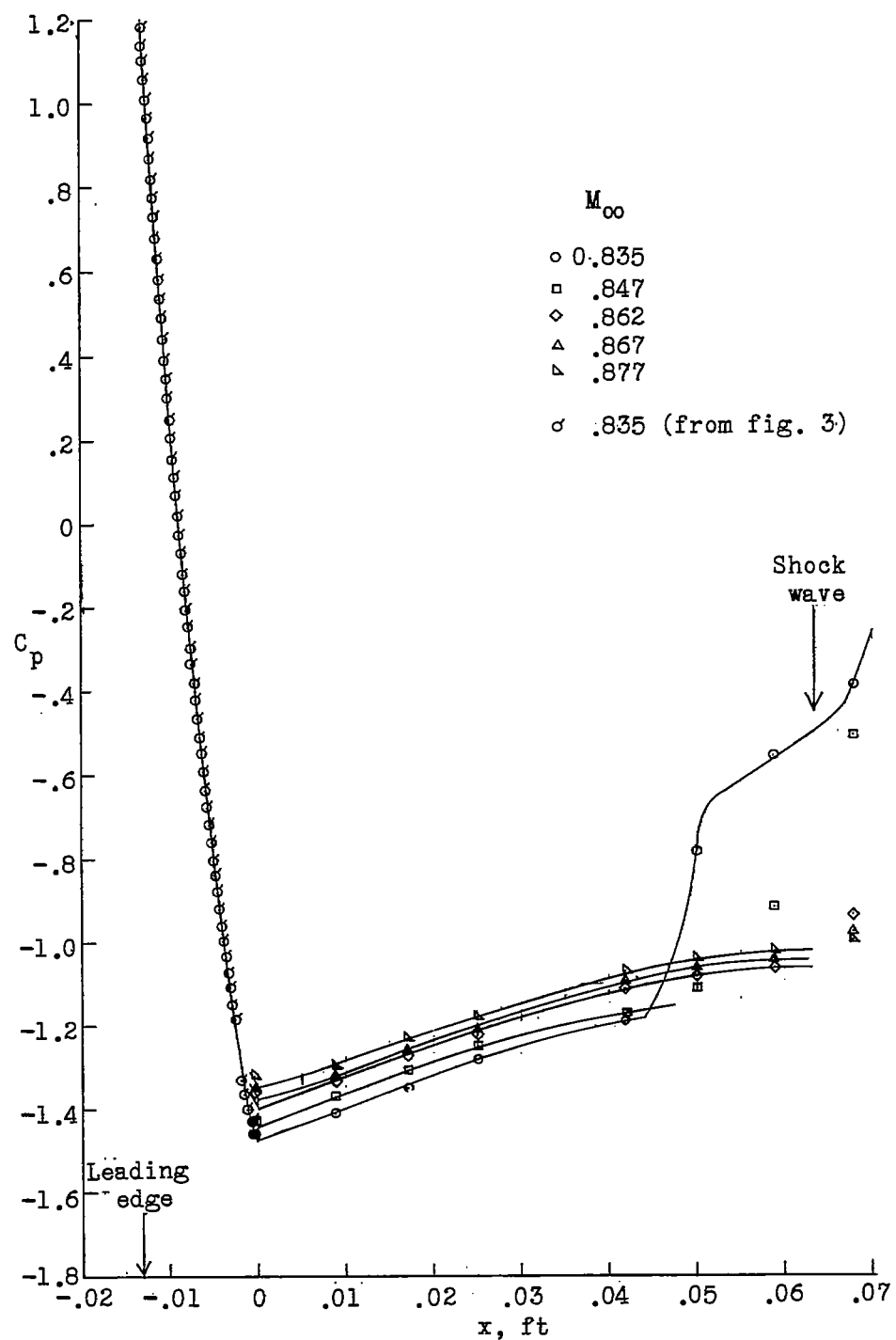
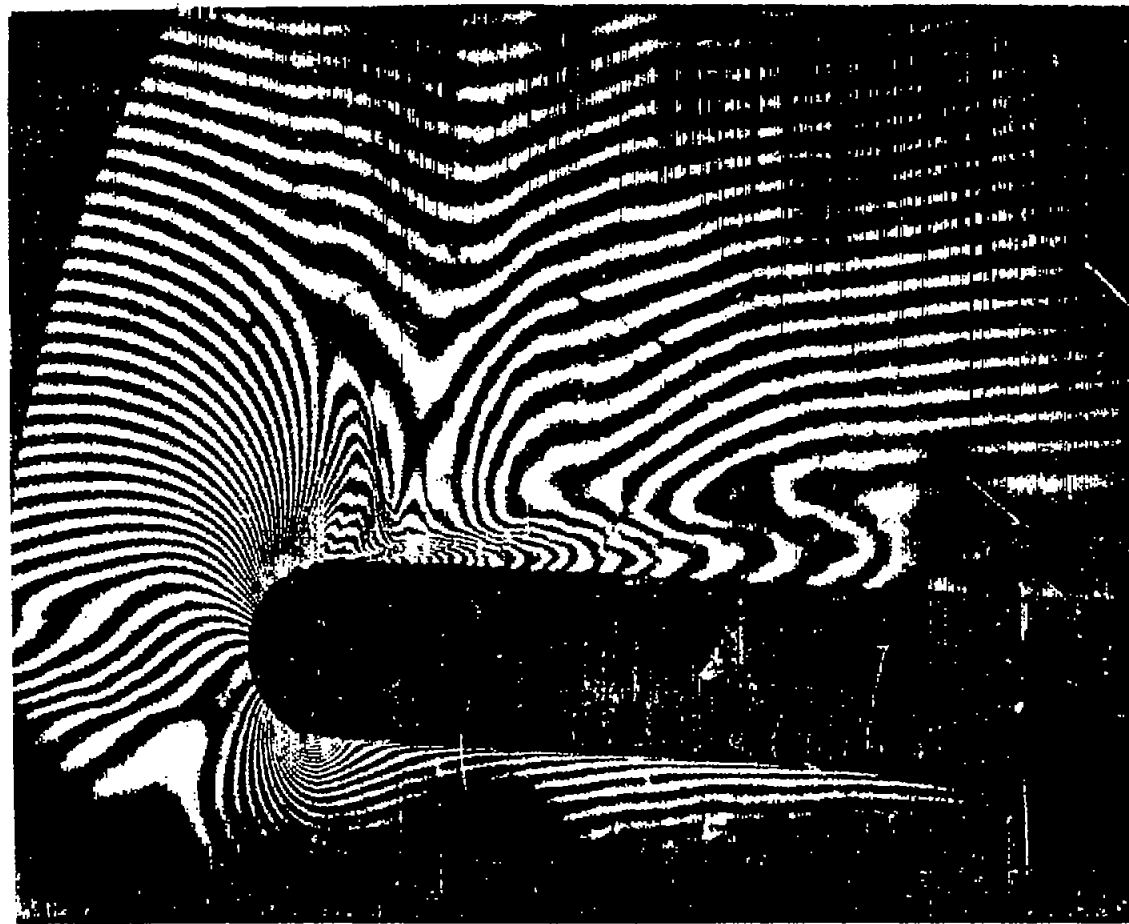
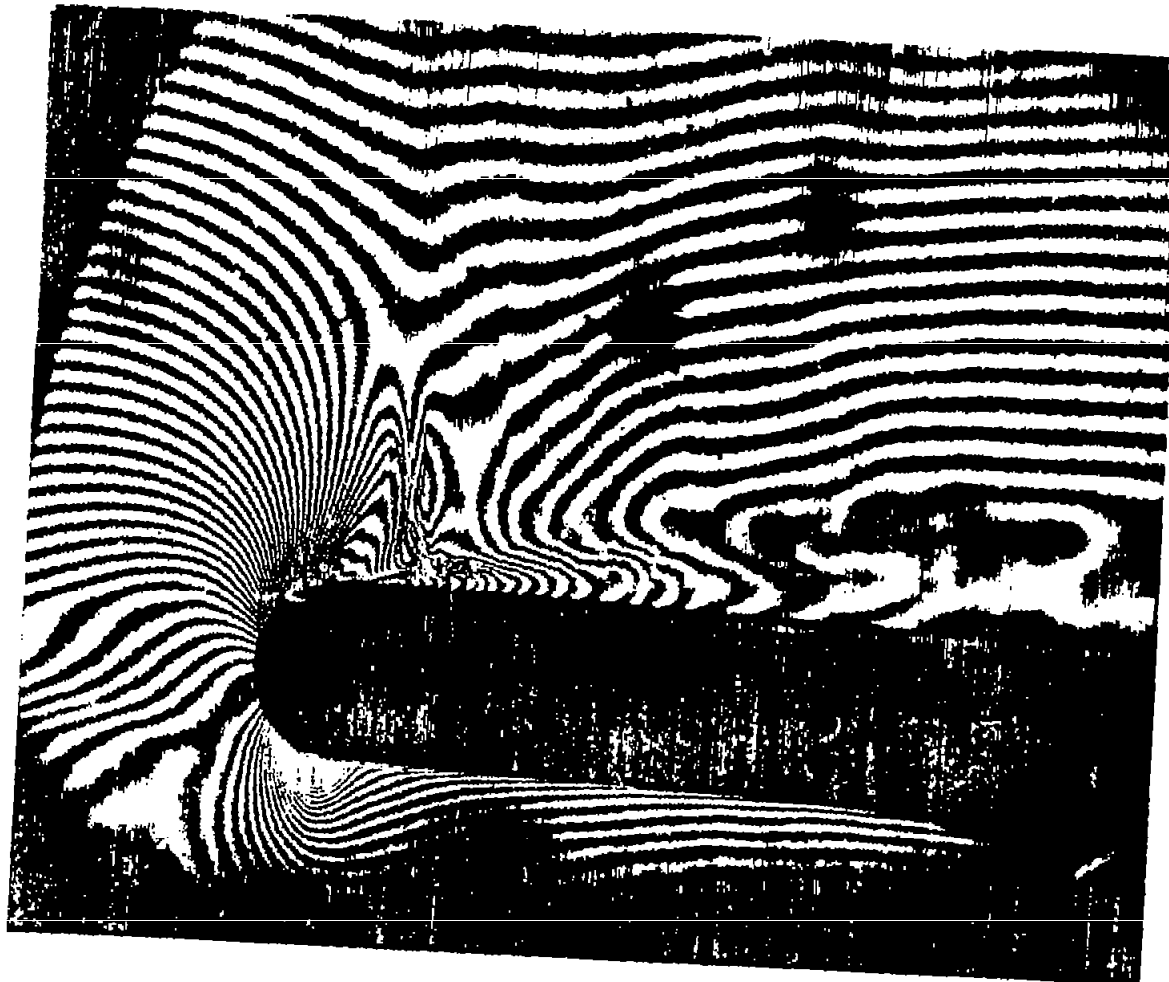


Figure 4.- Pressure distribution on model with attached flow at various Mach numbers.

(a) $M_\infty = 0.700.$

L-93563

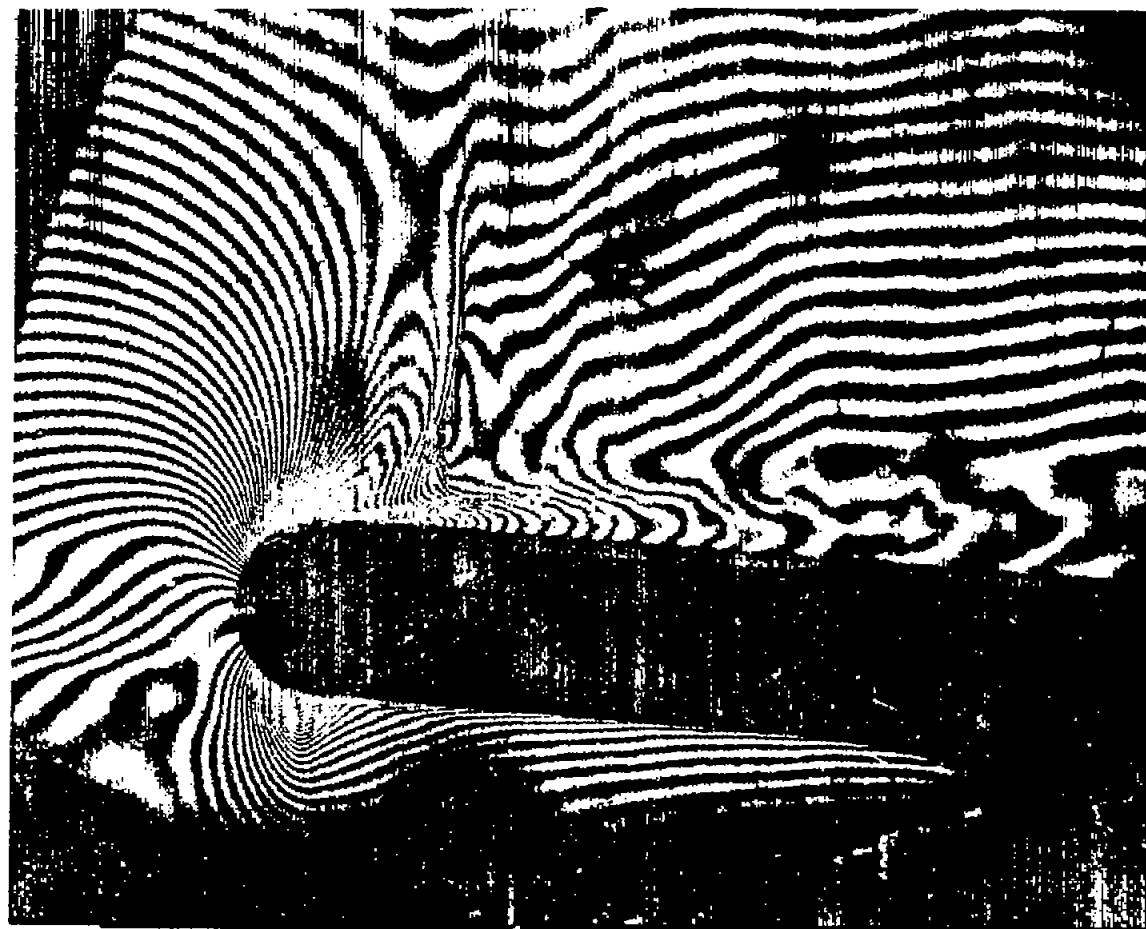
Figure 5.- Interferograms of the flow in the vicinity of the rounded leading edge of a flat plate 5/16 inch thick. Early transition of boundary layer was induced by wire ahead of model.



(b) $M_\infty = 0.719.$

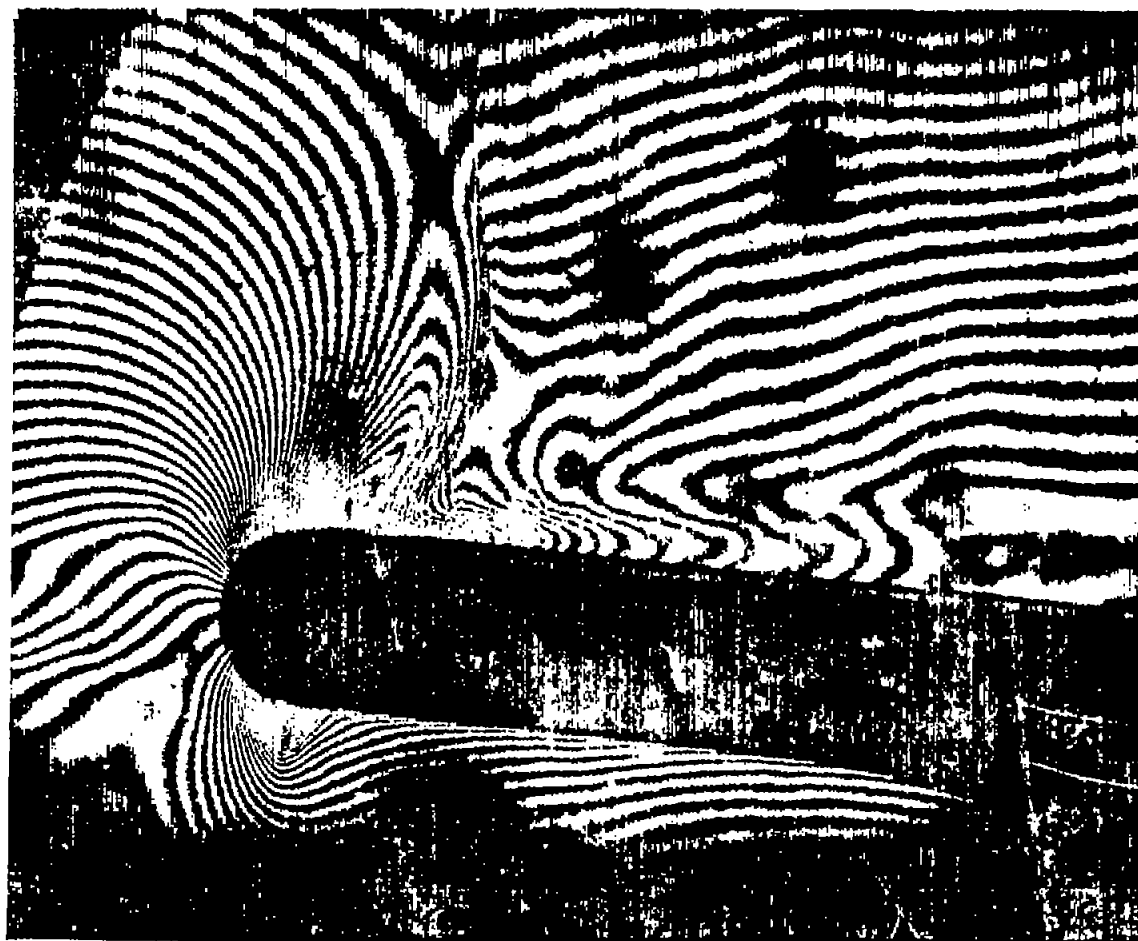
I-93564

Figure 5.- Continued.

(c) $M_\infty = 0.741.$

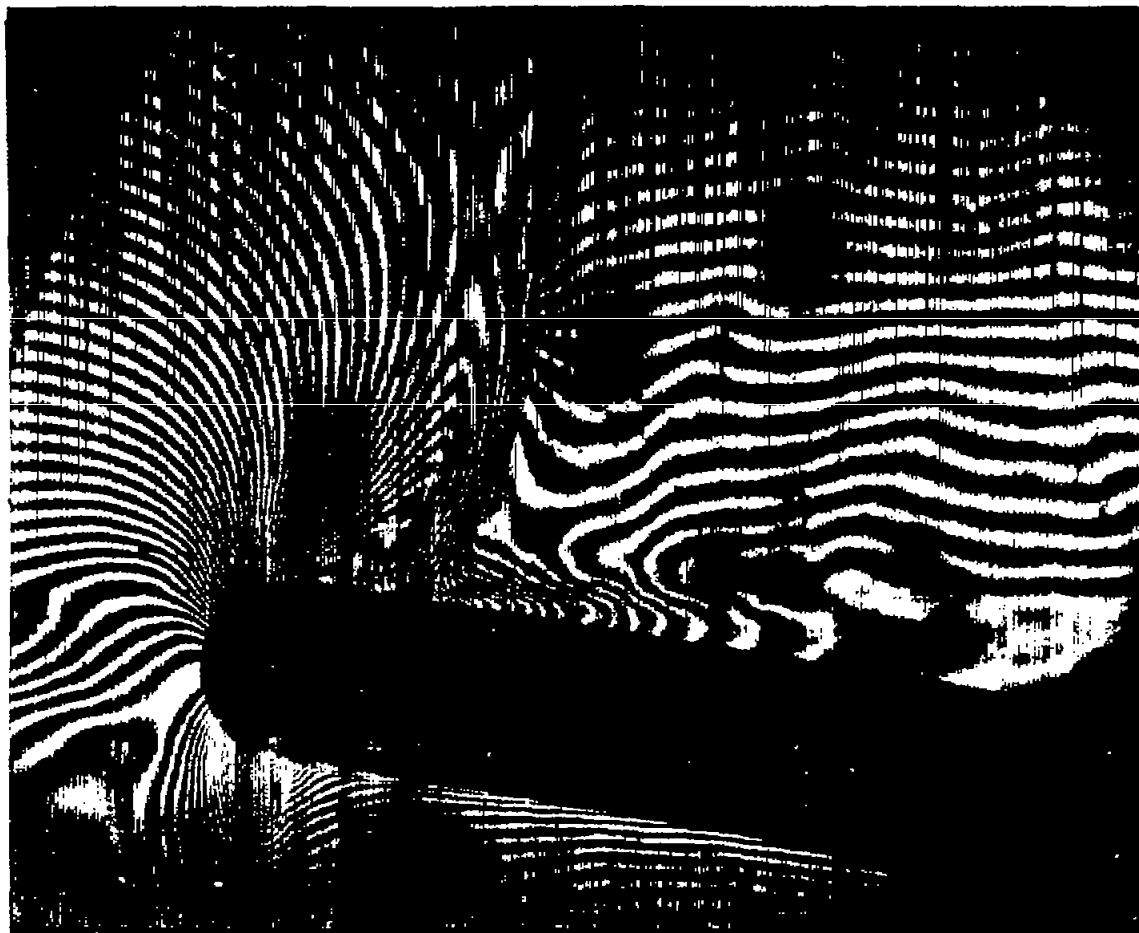
I-93565

Figure 5.- Continued.



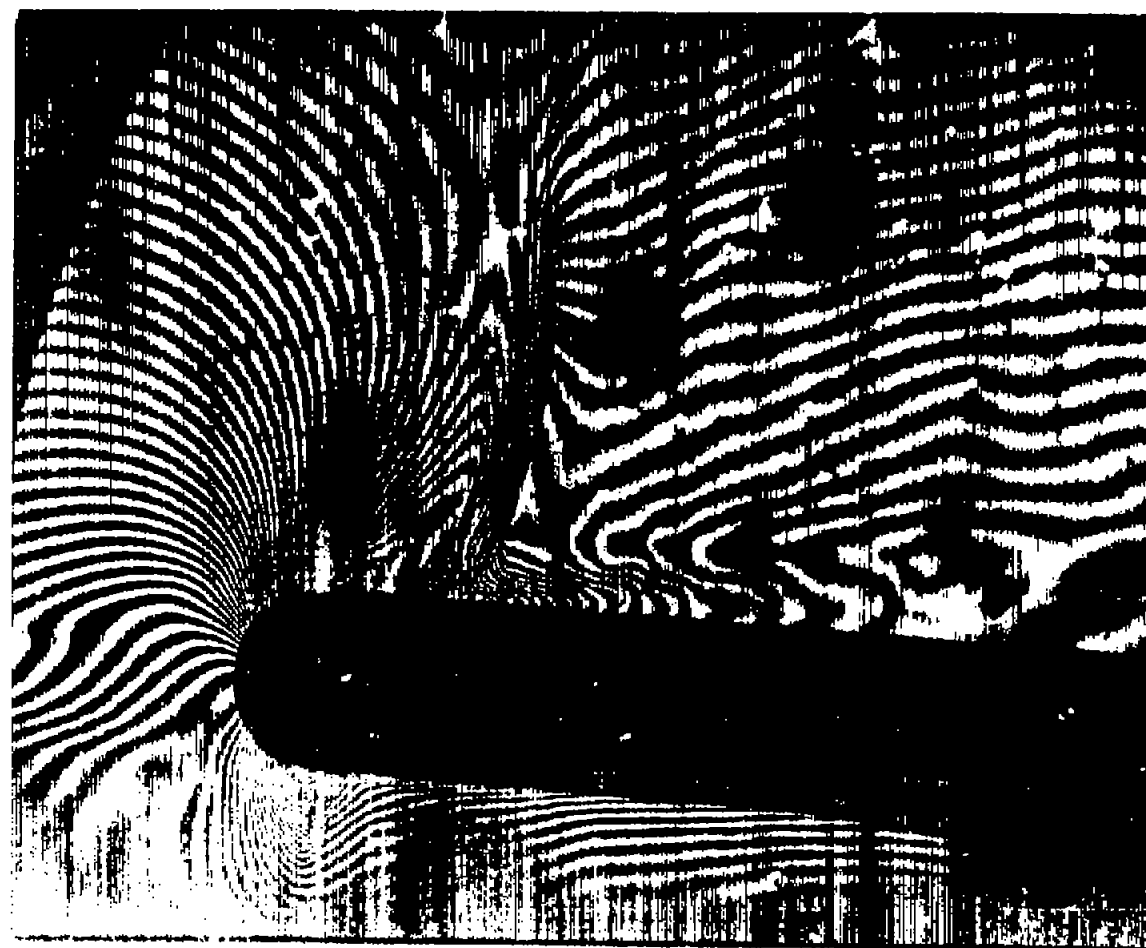
(d) $M_\infty = 0.751.$ I-93566

Figure 5.- Continued.

(e) $M_\infty = 0.762$.

L-93567

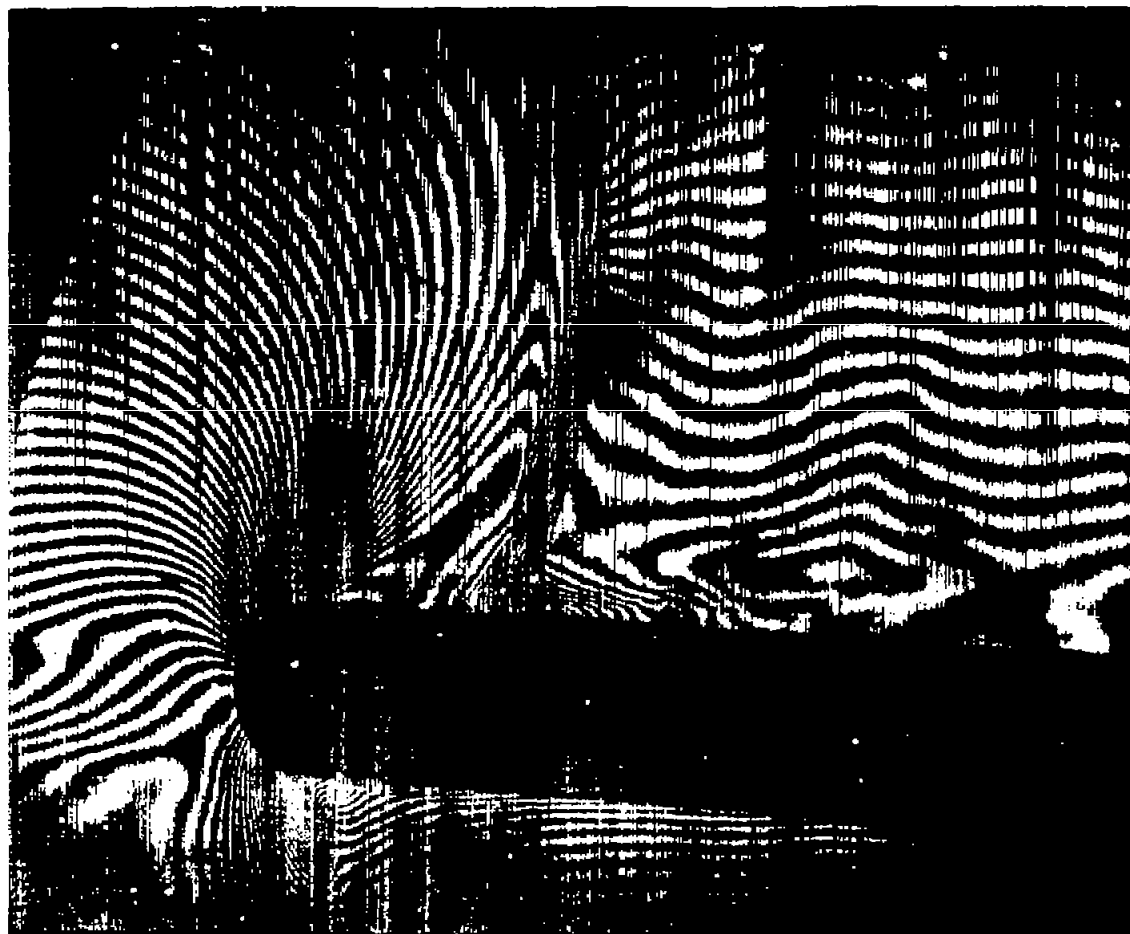
Figure 5.- Continued.



(f) $M_\infty = 0.769.$

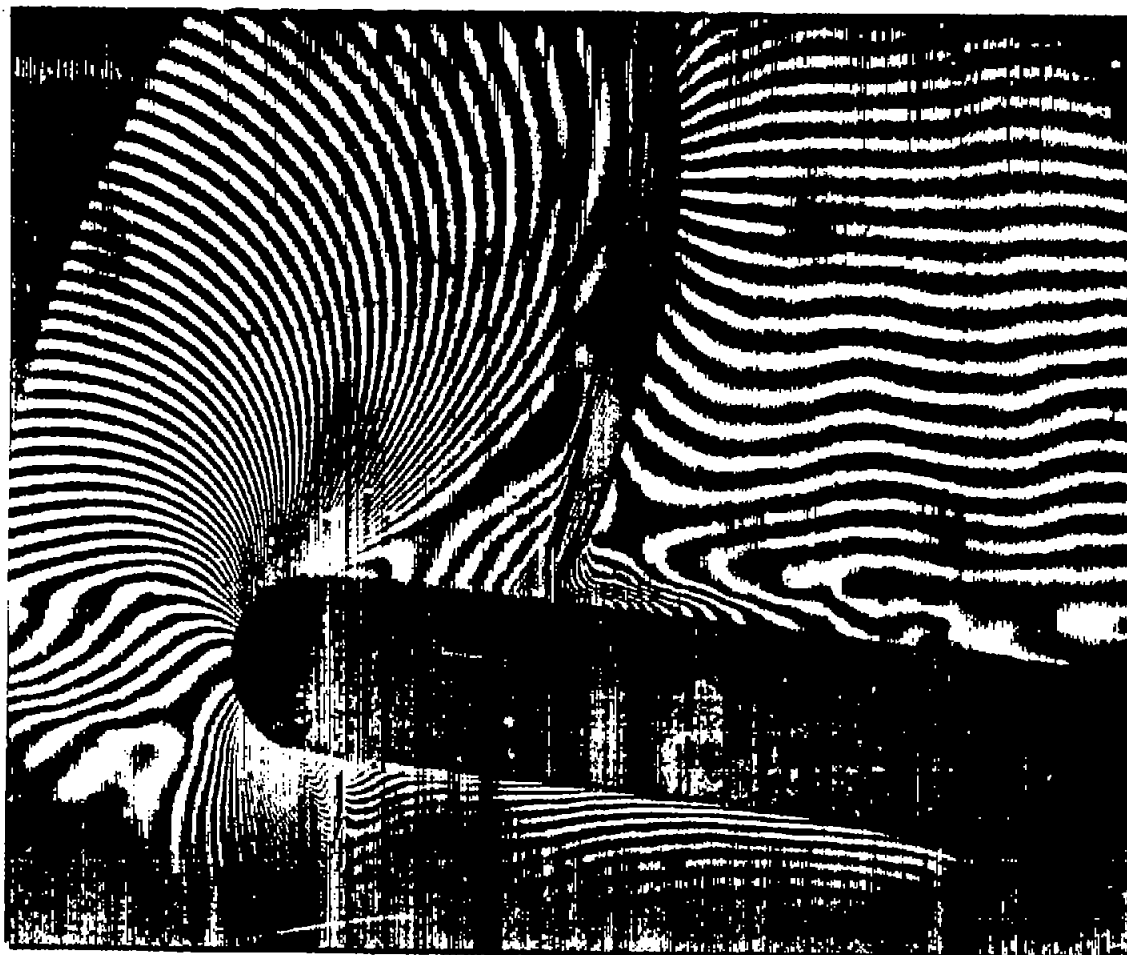
L-93568

Figure 5.- Continued.

(g) $M_\infty = 0.779$.

L-93569

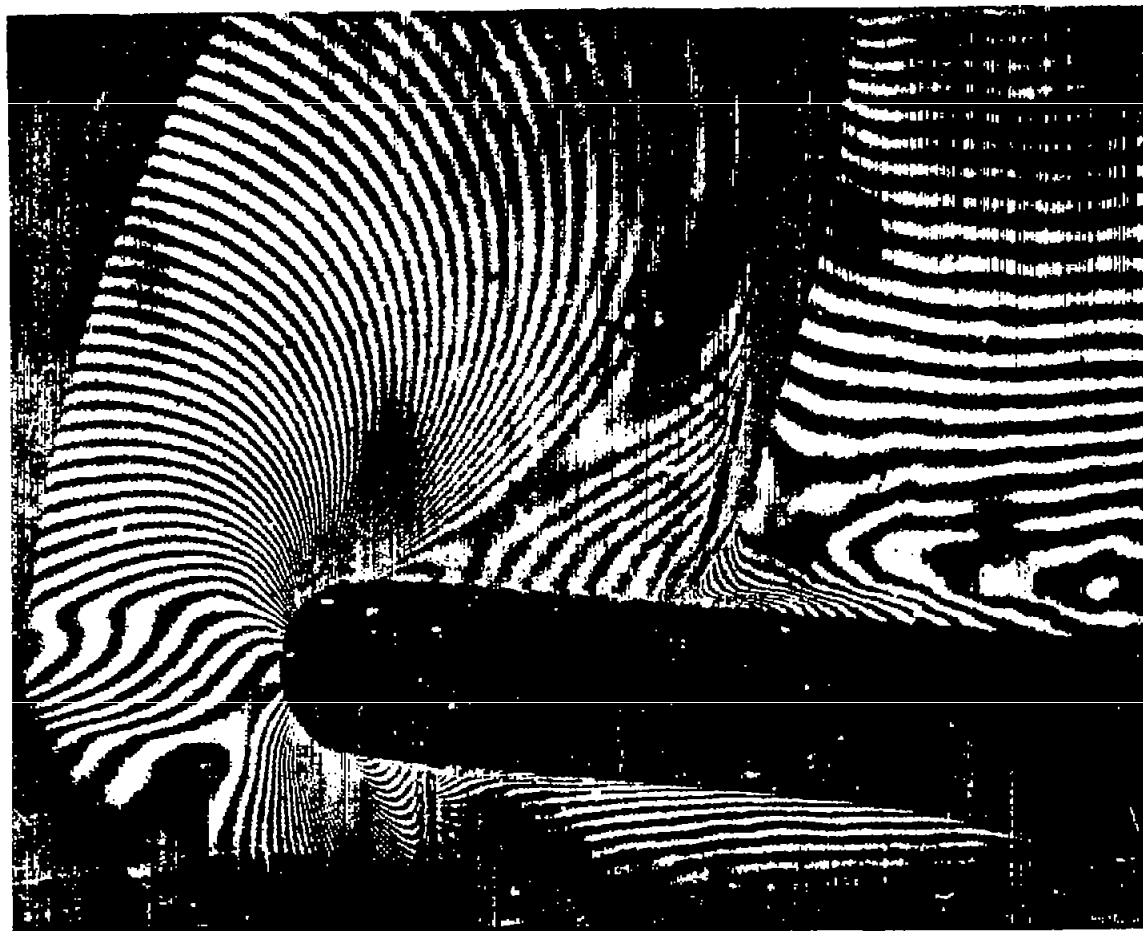
Figure 5.- Continued.



(h) $M_{\infty} = 0.798.$

I-93570

Figure 5.- Continued.

(i) $M_\infty = 0.833$.

L-93571

Figure 5.- Concluded.

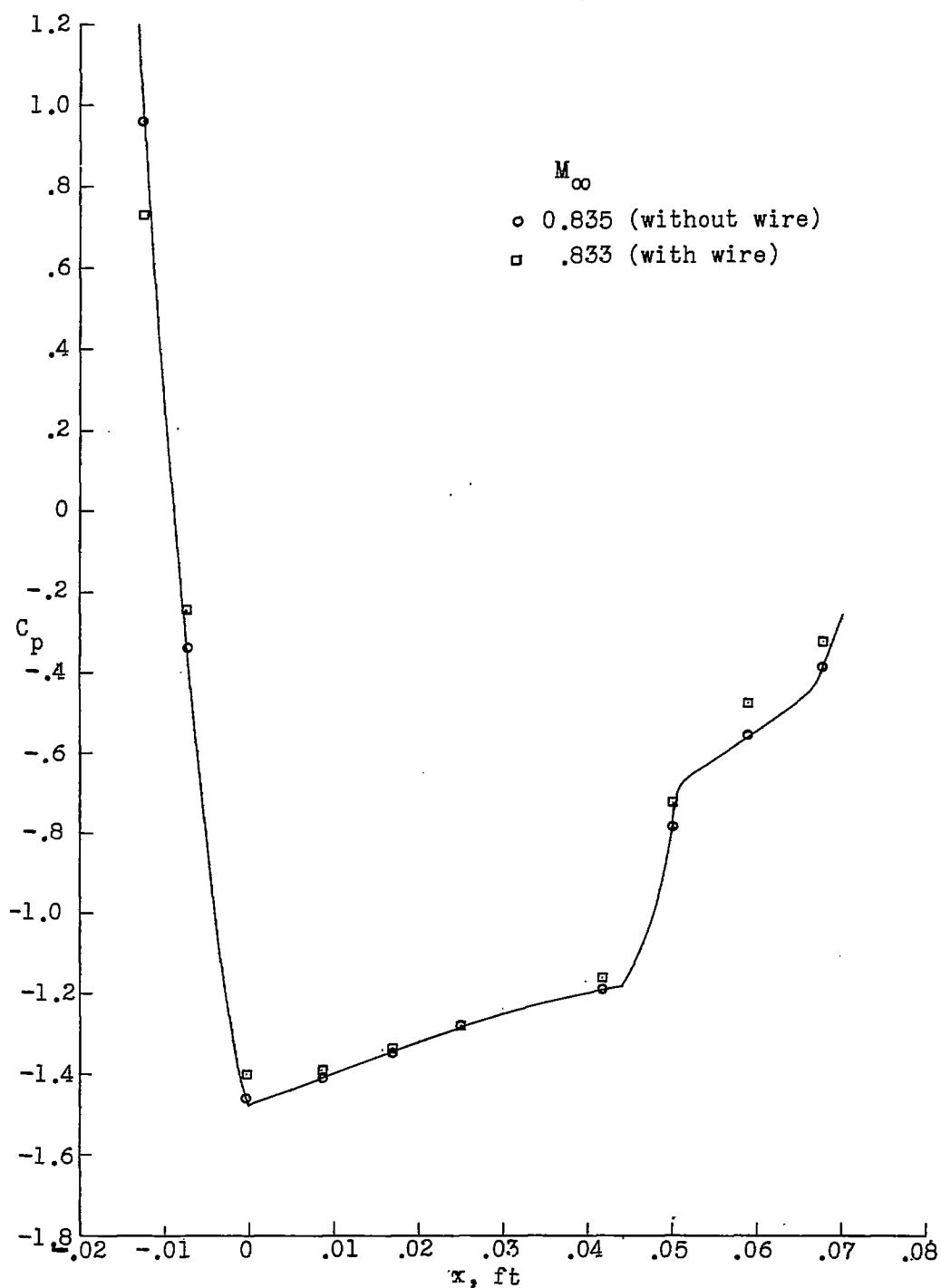


Figure 6.- Pressure distribution with and without turbulence-inducing wire.

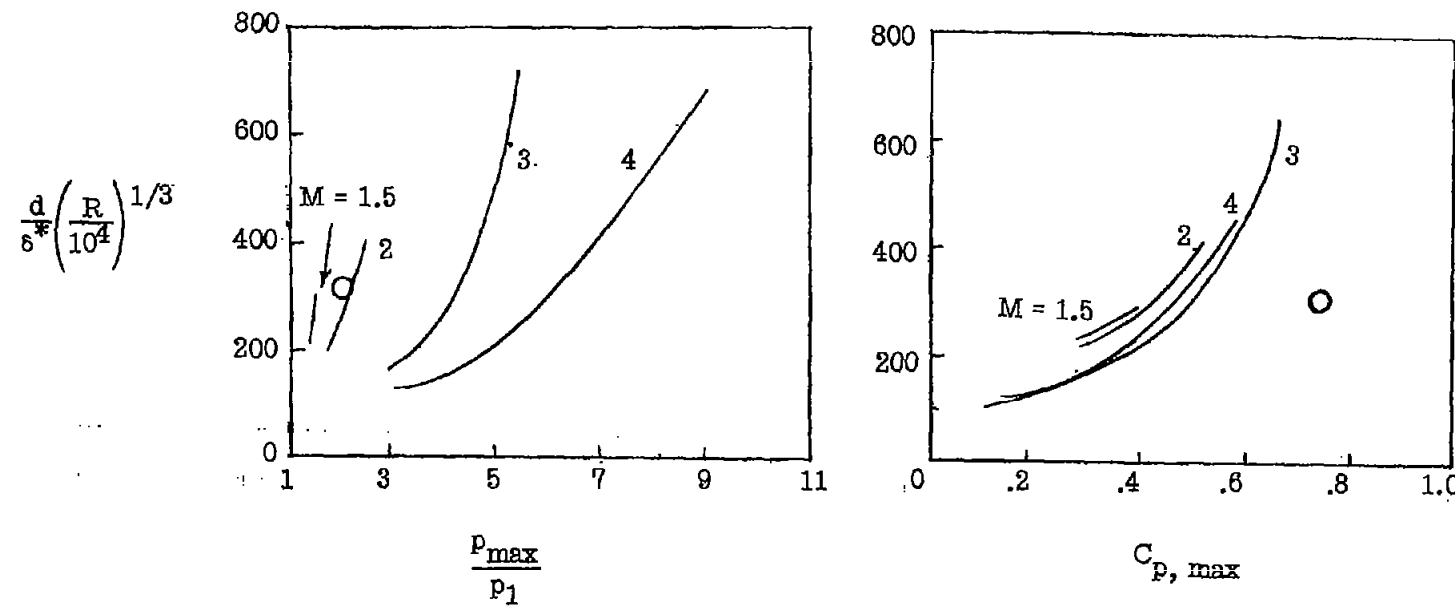


Figure 7.- Upstream influence distance. Laminar boundary layer; wedge in stream. From reference 6, except points shown by circles which represent results of present investigation. For the circles, $M = 1.5$ just ahead of base of shock wave.

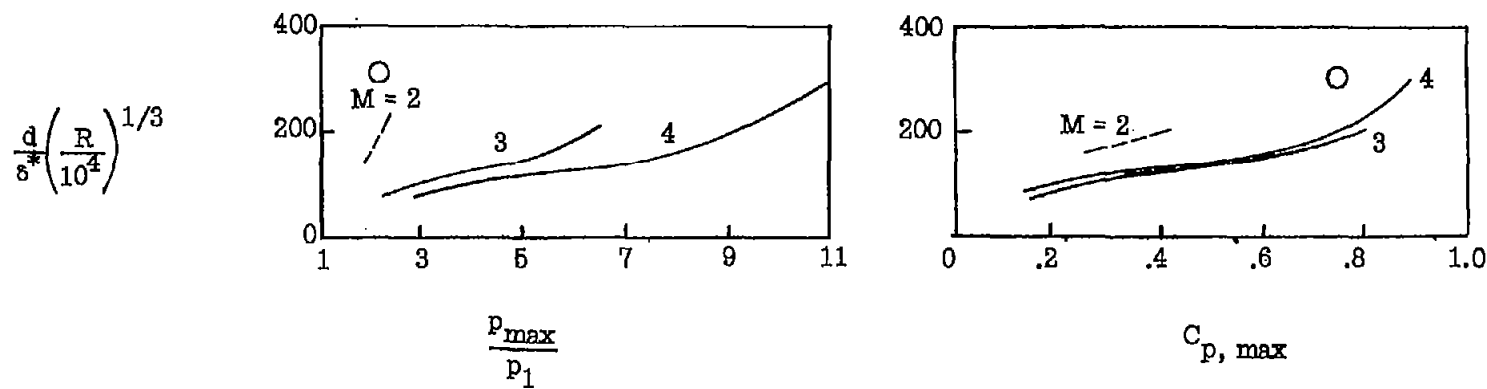


Figure 8.- Upstream influence distance. Laminar boundary layer; wedge on plate. From reference 6, except points shown by circles which represent results of present investigation. For the circles, $M = 1.5$ just ahead of base of shock wave.

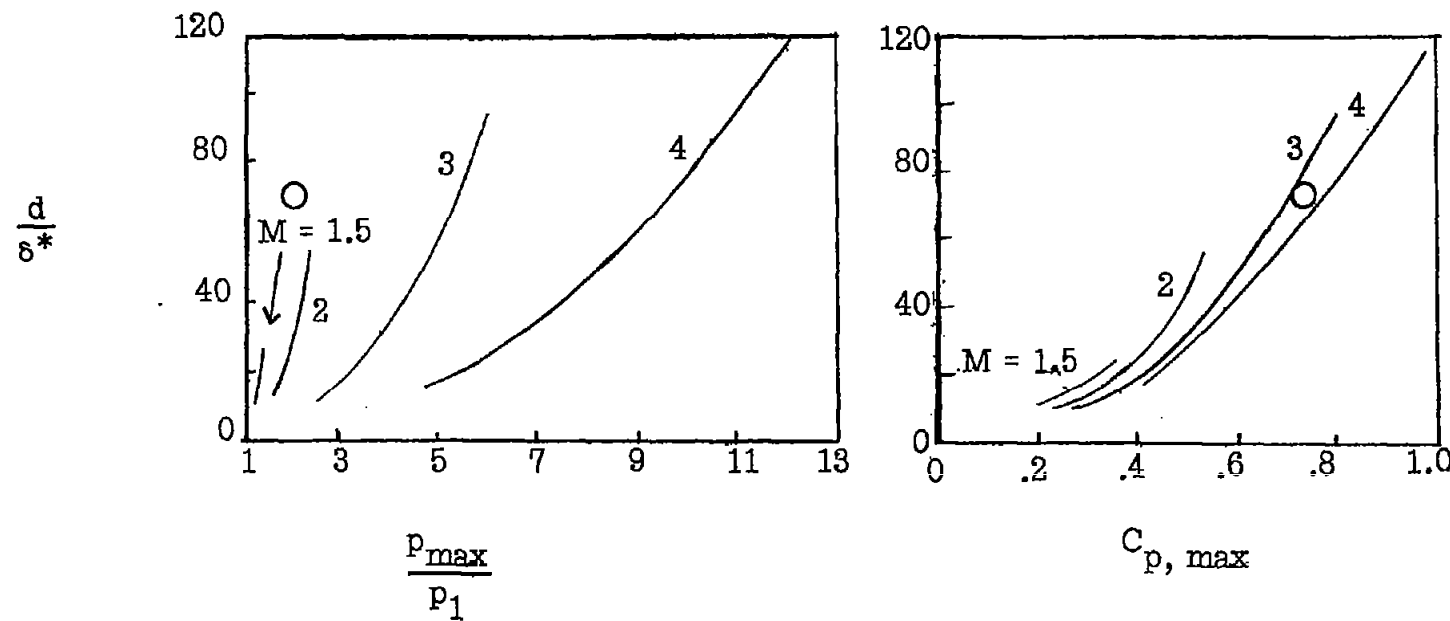


Figure 9.-- Upstream influence distance. Turbulent boundary layer; wedge in stream. From reference 6, except points shown by circles which represent results of present investigation. For the circles, $M = 1.5$ just ahead of base of shock wave.

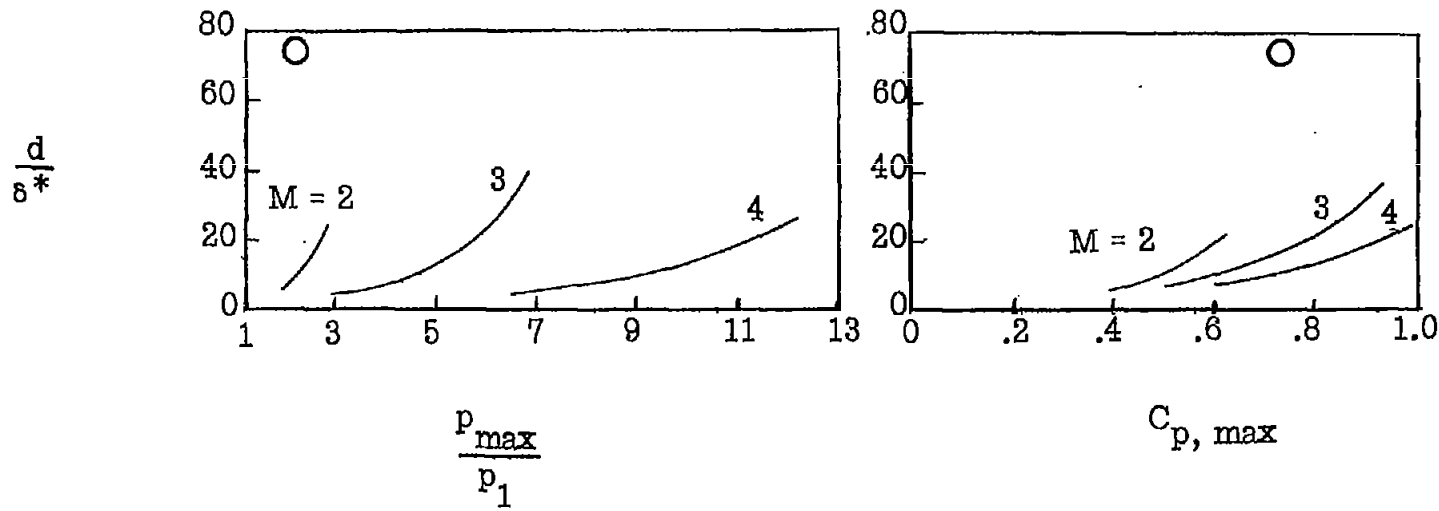


Figure 10.- Upstream influence distance. Turbulent boundary layer; wedge on plate. From reference 6, except points shown by circles which represent results of present investigation. For the circles, $M = 1.5$ just ahead of base of shock wave.